*diversity*

MDPI

*Article*

# Is a Modified Actin the Key to Toxin Resistance in the Nudibranch *Chromodoris*? A Biochemical and Molecular Approach

**Cora Hertzer [1,2,*], Nani Ingrid Jacquline Undap [3,4], Adelfia Papu [3,5], Dhaka Ram Bhandari [6,7], Stefan Aatz [8], Stefan Kehraus [1], Fontje Kaligis [9,†], Robert Bara [9], Till F. Schäberle [10], Heike Wägele [3] and Gabriele M. König [1]**

1 Institute for Pharmaceutical Biology, University of Bonn, Nussallee 6, 53115 Bonn, Germany
2 Cawthron Institute, 98 Halifax Street, The Wood, Nelson 7010, New Zealand
3 Leibniz Institute for the Analysis of Biodiversity Change, Museum Koenig Bonn, Adenauerallee 160, 53113 Bonn, Germany
4 Research Center for Conservation of Marine and Inland Water Resources, National Research and Innovation Agency, Bogor 16911, Jawa Barat, Indonesia
5 Faculty of Mathematics and Natural Sciences, Sam Ratulangi University, Jl. Kampus UNSRAT Bahu, Manado 95115, Sulawesi Utara, Indonesia
6 Institute of Inorganic and Analytical Chemistry, Justus-Liebig-University, Heinrich-Buff-Ring 17, 35392 Gießen, Germany
7 Gandaki Province Academy of Science and Technology (GPAST), Pokhara 33700, Nepal
8 Institute of Biochemistry and Molecular Biology, University of Bonn, Nussallee 11, 53115 Bonn, Germany
9 Faculty of Fisheries and Marine Science, Sam Ratulangi University, Jl. Kampus UNSRAT Bahu, Manado 95115, Sulawesi Utara, Indonesia
10 Institute for Insect Biotechnology, Justus-Liebig-University and Department for Bioresources of the Fraunhofer Institute for Molecular Biology and Applied Ecology, Ohlebergsweg 12, 35392 Gießen, Germany
* Correspondence: cora.hertzer@cawthron.org.nz
† Fontje Kaligis: deceased.



**Citation:** Hertzer, C.; Undap, N.I.J.; Papu, A.; Bhandari, D.R.; Aatz, S.; Kehraus, S.; Kaligis, F.; Bara, R.; Schäberle, T.F.; Wägele, H.; et al. Is a Modified Actin the Key to Toxin Resistance in the Nudibranch *Chromodoris*? A Biochemical and Molecular Approach. *Diversity* **2023**, *15*, 304. https://doi.org/10.3390/d15020304

Academic Editors: Giulia Furfaro and Paolo Mariottini

Received: 1 December 2022
Revised: 26 January 2023
Accepted: 10 February 2023
Published: 18 February 2023



**Abstract:** Five *Chromodoris* species from North Sulawesi, Indonesia, were investigated for their sequestration of marine natural products. The cytotoxic 2-thiazolidinone macrolide latrunculin A (LatA) was the major metabolite in all examined *Chromodoris* species, as well as in one of the associated sponges *Cacospongia mycofijiensis* (Kakou, Crews & Bakus, 1987), supporting a dietary origin of LatA. Furthermore, LatA was secreted with the mucus trail, suggesting a possible use in short-range chemical communication. MALDI MS-Imaging revealed an accumulation of LatA throughout the mantle tissue, mucus glands, and especially in vacuoles of the mantle dermal formations (MDFs). Cytotoxicity of the isolated LatA was tested in HEK-293 cells, confirming that LatA targets the actin cytoskeleton. *In vivo* toxicity experiments with the sacoglossan *Elysia viridis* (Montagu, 1804) showed 100% mortality, but 100% survival of *Chromodoris* specimens, demonstrating resistance to LatA. A novel actin isoform was detected in all investigated *Chromodoris* species with two amino acid substitutions at the 'nucleotide binding' cleft, the binding site of LatA. These are suggested to cause insensitivity against LatA, thus enabling the storage of the toxin within the body for the slugs' own defense.

**Keywords:** actin; *Chromodoris*; cytotoxic; heterobranchia; latrunculin; nudibranchia; resistance

## 1. Introduction

Nudibranchia sea slugs (Gastropoda, Mollusca) have completely reduced their shell [1]. This represents several advantages, such as less energetic costs of developing and transporting a shell, as well as other respiratory and excretory benefits [2,3]. However, the exposed soft body makes them more susceptible to predation [4–8], which is compensated for by developing elaborate defense strategies. In particular, the selective uptake, sequestration and storage of toxic chemicals from their prey is considered a very effective defense system.

This is well-studied in many nudibranch sea slugs, including the colorful Chromodorididae (Doridina) [3,9–15]. Their aposematic colors and patterns are assumed to be part of Müllerian and quasi-Batesian mimicry with other slugs or metazoan life forms [16–20]. So far, the only observed predation on *Chromodoris* nudibranchs has been by the carnivorous dorid nudibranch genus *Gymnodoris* [21].

Currently, 22 described and other putative 18 undescribed *Chromodoris* species are distributed throughout the Indo-Pacific Ocean and the Red Sea [17]. However, species delimitation for this genus is subject to ongoing research due to unique challenges, such as extraordinary cryptic diversity, mimicry and recent radiation with described introgression, mitochondrial capture and hybridization, and could therefore undergo further revisions [16–19]. Of these putative 40 *Chromodoris* species, 12 have been chemically investigated and were included in several reviews [3,12–14,22]. They all contained diet-derived, bioactive, often cytotoxic, marine natural products (MNPs) with variations in relation to prey availability. The MNPs play key roles, not only as a defense against predators, pathogens and overgrowth by fouling organisms, but also as semiochemicals for inter- and intra-specific communication, in reproduction and development [3,9,23–33]. Therefore, they can be traced in certain body parts, in the epidermis, mantle tissue and mantle dermal formations (MDFs, Figure 1B,C), and even in the mucus of the slugs. Most notable is the selective uptake and storage of the cytotoxins latrunculin A (LatA, Figure 1A) and latrunculin B (LatB) by *Chromodoris* species [11]. Until now, the incorporation of latrunculins has been reported only for this heterobranch genus [11,34–39], and here especially for Australian *Chromodoris annae* Bergh, 1877, *C. elisabethina* Bergh, 1877, *C. kuiteri* Rudman, 1982, *C. lochi* Rudman, 1982, and *C. magnifica* (Quoy & Gaimard, 1832) [11,15,35,37,39], South and East African *C. hamiltoni* Rudman, 1977 [36,40], as well as *C. quadricolor* (Rüppell & Leuckart, 1830) [41,42], and *C. africana* Eliot, 1904 from the Red Sea [43]. Usually, the sponges of the genera *Negombata* and *Cacospongia*, which serve as food sources for *Chromodoris* nudibranchs, are considered as the source of latrunculins, especially LatA [44].

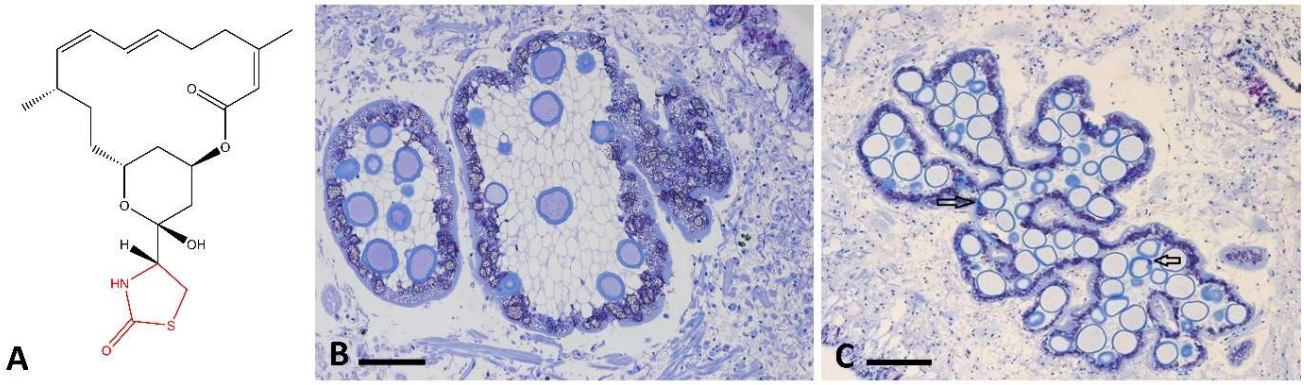


**Figure 1.** (**A**) Chemical structure of latrunculin A (LatA). The rare 2-thiazolidinone moiety is indicated in red. (**B**) Mantle dermal formation (MDF) of *Chromodoris lochi*. (**C**) MDF of *Chromodoris annae*. Arrows indicate the nucleus of a glandular cell inside the MDF. Scale bar: 100 µm.

Latrunculins are cytotoxic 14- and 16-membered macrolides with an attached rare 2-thiazolidinone moiety (Figure 1), derived from mixed polyketide synthase/non-ribosomal peptide synthetase (PKS-NRPS) biogenesis and are unique to the marine environment [44,45]. They have been studied for more than 40 years, especially with regard to their mechanism of action and potential for therapeutic applications [38,44,46–83]. This substantial interest in latrunculins is primarily based on their actin filament depolymerizing effect and LatA has become the most widely used small molecule to study actin-based processes, microfilament organization, cytoskeleton dynamics, mechanisms of cellular function and the potential of latrunculins as a treatment against cancer, neurological disorders and infectious diseases [51,55,66,72,79,82,84].

Actins are highly conserved proteins that are ubiquitously expressed in every eukaryotic cell. They play key roles in cytoskeleton formation, movement, intracellular transport, transcriptional regulation and DNA replication [85–97]. However, their vital importance, evolutionary age and high conservation make them a perfect target for toxins. Several organisms have evolved the ability to produce or acquire actin-targeting toxins, thus ensuring effectiveness, even lethality, against a broad spectrum of organisms [72,82,84,98]. Latrunculins are unique in their bioactivity because they are the only currently known toxins that bind to the 'nucleotide binding' cleft of G-actin (Figure 2, SI Table S3) [51,55,60,72,79,90]. Previous studies have shown that one amino acid mutation of G-actin is enough to cause resistance to latrunculins. Up to now, fifteen actin amino acid positions have been identified, which can cause latrunculin resistance when mutated (SI Table S3) [51,52,55,60,99–105].

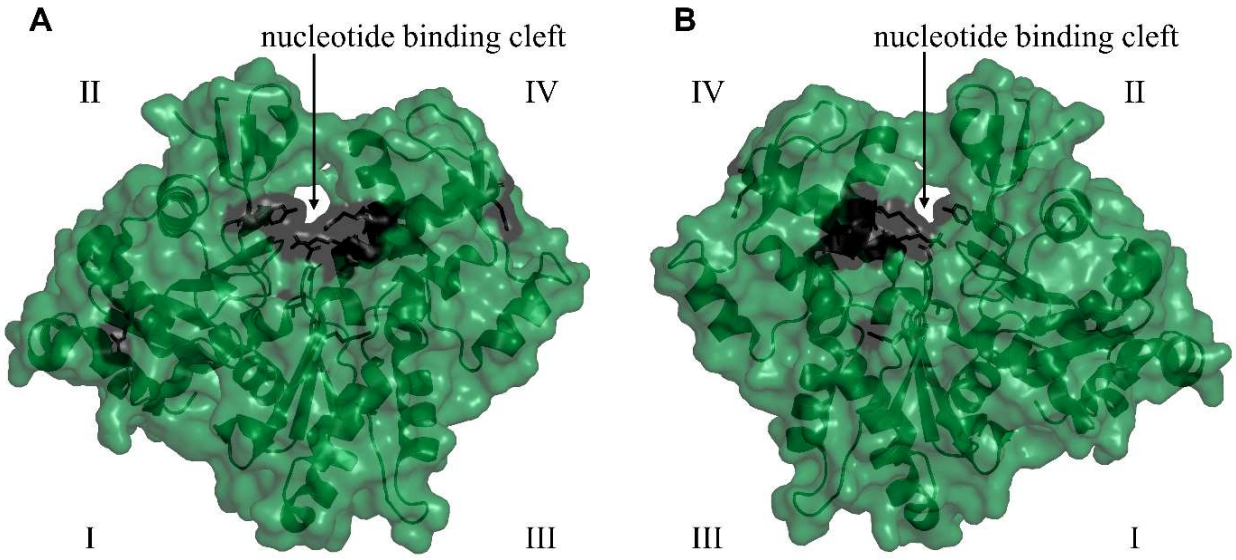


**Figure 2.** Surface model of native G-actin and its subdomains I–IV (green, PDB: 3HBT) with reported sites of amino acid mutations (black), each leading to the inhibition of latrunculin binding (see SI Table S3). (**A**,**B**) Front and back view of G-actin.

So far, it is unknown how heterobranch sea slugs can withstand the toxicity of actin-binding toxins. This is also true for LatA, its effect on actins within *Chromodoris* nudibranchs, and how they avoid autotoxicity. Organisms that produce or acquire toxic natural products must be resistant to the action of these substances to gain an advantage [106–110]. One way to avoid autotoxicity is to use compartmentalization, or (sub)cellular localization, where toxins are concentrated in vesicles, vacuoles, compartments or glands. The compartmentalization of cytotoxic compounds has frequently been observed in sponges, including the food of *Chromodoris* species, *Negombata* [81,111–119].

Chromodorididae have been found to store higher concentrations of sequestered secondary metabolites in specialized globular storage glands in the mantle tissue, composed of cells with large, non-staining vacuoles: the so-called mantle dermal formations (MDFs) (Figure 1B,C) [1,39,120–125]. These MDFs are highly concentrated chemical packages, deterring predators which might not have been deterred by lower concentrations of the metabolites when uniformly distributed in the mantle [126]. The MDFs are situated in the outer area of the mantle, the mantle rim, which is often bright or aposematically colored, drawing the predators' attention towards this well-defended area [11,125–128]. The evolution of defensive mantle glands and MDFs is considered a key innovation that has contributed to the extensive radiation and speciation of the Chromodorididae [127]. However, the storage of secondary metabolites and the defensive role of MDFs might have evolved secondarily to their primary function as excretory or detoxification organs, expelling toxic substances and avoiding autotoxicity [1,123,124,126,129]. The secretion of

toxic waste material by mantle glands or its accumulation in MDFs might be an additional selective advantage against predation in combination with the prevention of autotoxicity.

Here, we investigate the sequestration and distribution of LatA in five *Chromodoris* species: *Chromodoris annae*, *C. dianae* Gosliner & Behrens, 1998, *C. lochi*, *C. strigata* Rudman, 1982 and *C. willani* Rudman, 1982 (Figure 3A–E). Additionally, we examine a possible underlying molecular resistance mechanism in these nudibranchs, a prerequisite that would allow them to sequester, survive and store the cytotoxin LatA. Our key objectives in this study were to: (1) chemically investigate and characterize the major metabolite in all five *Chromodoris* species, and their putative prey *Cacospongia mycofijiensis* (Thorectidae, Porifera); (2) visualize the cross-sectional distribution of the main metabolite LatA in *C. annae* and *C. dianae* nudibranchs by MALDI MSI; (3) examine and compare LatA's toxicity and mode of action in HEK-293 cells, and *in vivo* in *Chromodoris* and *Elysia viridis* (Figure 3F) heterobranchs; and (4) investigate a possible molecular resistance mechanism in *Chromodoris* nudibranchs, by comparison of actin nucleotide and amino acid sequences obtained for *Chromodoris* species, with further heterobranch members, the sacoglossan *Elysia viridis*, the anaspidean *Aplysia californica* J. G. Cooper, 1863, and the three cladobranch species *Flabellina affinis* (Gmelin, 1791), *Embletonia pulchra* (Alder & Hancock, 1844), and *Armina tigrina* Rafinesque, 1814.

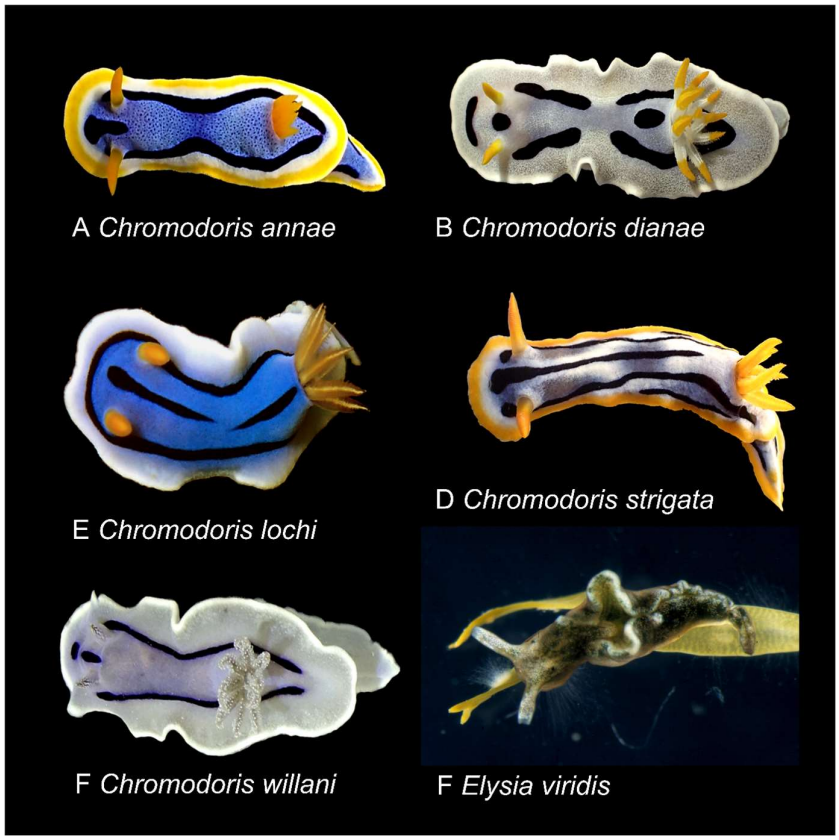


**Figure 3.** Photographs of the investigated *Chromodoris* species (**A**–**E**) and *Elysia viridis* (**F**).

## 2. Materials and Methods

### *2.1. Biological Material*

The origin and further use of the individuals in the corresponding experiments are summarized in Table 1. Specimens for chemical analyses were collected via scuba diving from various sponge substrates between 2015 and 2018 and preserved in 98% EtOH. The mucus of *Chromodoris annae* was collected by cleaning bowls with tissue, where slugs have crawled and by patting the notum of the animals with a small piece of tissue. This tissue was separately preserved in 98% EtOH. Eight specimens of *C. annae* and five *C. dianae* (5)

were used for chemical comparison of the mantle rim, including the MDFs, and the rest of the body. For this purpose, the mantle rim was dissected away from the rest of the body. These parts were stored separately at −20 °C after fixation in 96% EtOH until further extraction and processing in the laboratories at the University of Bonn. Live animals for the MALDI imaging experiments were first kept in aerated aquaria matching the temperature, salinity and density of the Indo-Pacific Ocean, before the single available *C. dianae* specimen was snap-frozen with liquid nitrogen and stored at −80 °C, and the two *C. annae* specimens were frozen in seawater.

**Table 1.** Species names and further details of the specimens analyzed in this study, and the experiments in which the specimens were used. BNP Bunaken National Park, North Sulawesi.

| Experiment/Involved Species and Sizes | Number of Specimens Used in Respective Experiment | Locality | Fixation | Further Treatment |
|---|---|---|---|---|
| *Chemical analysis* | | | | |
| *Chromodoris annae* (20–45 mm) | 58 | BNP 2015/16 | 96% EtOH | Whole animals |
| *C. annae* (20–27 mm) | 6 | Sangihe 2016 | 96% EtOH and stored at −20 °C | Before fixation mantle rim and rest of body separated |
| *C. annae* mucus | several | Bangka Island 2019 | 96% EtOH | |
| *Chromodoris dianae* (20–55 mm) | 56 | BNP 2015/16 | 96% EtOH | Whole animals |
| *C. dianae* (27–45 mm) | 6 | Sangihe 2016 | 96% EtOH and stored at −20 °C | Before fixation mantle rim and rest of body separated |
| *Chromodoris lochi* (15–50 mm) | 31 | BNP 2015/16 | 96% EtOH | Whole animals |
| *Chromodoris willani* (20–70 mm) | 32 | BNP 2015/16 | 96% EtOH | Whole animals |
| *Chromodoris strigata* (20–25 mm) | 2 | Bangka Island 2019 | 96% EtOH | Only preservation fluid |
| *MALDI-MS Imaging* | | | | |
| *C. annae* | 2 | BNP 2017 | Frozen in seawater (−20 °C) | Stored at –20 °C |
| *C. dianae* | 1 | BNP 2017 | Brought alive to Germany, then snap-frozen in liquid nitrogen | |
| *In Vivo Toxicity Assay* | | | | |
| *C. annae* (30 mm) | 1 | BNP 2018 | Brought alive to Germany | Kept in aquaria for 2 days before and after experiments |
| *C. dianae* (35, 43 mm) | 2 | BNP 2018 | Brought alive to Germany | Kept in aquaria for 2 days before and after experiments |
| *Elysia viridis* (10–12 mm) | 12 | Figueira da Foz, Portugal, 2018 | Brought alive to Germany | Kept in aquaria with *C. fragile* as food for 2 days before and after experiments, where appropriate |

*In vivo* toxicity experiments were performed with live *C. annae*, *C. dianae* and *Elysia viridis*, the latter kindly provided by C. Greve from the Mediterranean Sea. They were also kept in aerated aquaria under their respective conditions until further experiments were conducted. For details, see below. The nudibranchs were identified by H. Wägele, N. Undap and A. Papu at Sam Ratulangi University or at the Leibniz Institute for the Analysis of

Biodiversity Change, Museum Koenig, Bonn, Germany [130,131]. The sponge was identified as *Cacospongia mycofijiensis* using methods described by Ackers et al. [132]; see also Erpenbeck et al. [133].

When not completely used for the analyses, the specimens or part of the material is now stored at the Sam Ratulangi University in the Reference Collection under the numbers SRU2015/01, SRU2016/02, SRU2017/1, SRU2018/1.

### 2.2. Chemical Analysis

Chemical analyses were performed at the University of Bonn.

*Extraction and Isolation.* Preserved *Chromodoris annae*, *C. dianae*, *C. lochi* and *C. willani* specimens were separated into species and location groups. They were separately frozen, crushed, and ultrasonicated (30 s intervals) on ice, while submerged in a minimum of first acetone (AC) and consecutively methanol (MeOH). Ethanolic storage solutions were each combined with the respective AC/MeOH extracts and dried under vacuum to give the crude extracts. Crude extracts were analyzed using HR-ESI-LCMS. Afterward, crude extracts were separated, using liquid–liquid separation, between water ($H_2O$) and three times ethyl acetate (EtOAc). The EtOAc-solubles were again analyzed by HR-ESI-LCMS. Location groups, of the same species, with a similar MS profile were combined and further separated by RP-HPLC. A Macherey-Nagel Nucleodur $C_{18}$ Pyramid column (250 mm × 10 mm; 5 µm), with isocratic gradient elution, 82:18 (MeOH:$H_2O$), and a flow of 1.0 mL/min were used for separation. The isolated main metabolite (LatA) had a retention time of around 41 min.

The dissected tissues of eight *C. annae* and five *C. dianae* were separately extracted as described above. Crude- and EtOAc-extracts of the mantle and body tissues were analyzed using HR-ESI-LCMS. Additionally, ethanolic storage solutions of *C. strigata*, and mucus collected with cellulose from the notum and foot of alive *C. annae* specimen, were examined using HR-ESI-LCMS. For further information see supplementary information.

*General Experimental Procedures.* Optical rotations were measured with a Jasco DIP 140 polarimeter. All NMR spectra were acquired in MeOH-$d_4$ using the Bruker Avance 300 DPX spectrometer. Spectra were referenced to residual solvent signals with resonances at $\delta_{H/C}$ 3.35/49.00 (MeOH-*d*4). Mass spectra were recorded on a micrOTOF-Q mass spectrometer (Bruker) with ESI-source coupled with an HPLC Dionex Ultimate 3000 (Thermo Scientific) using an Agilent Zorbax Eclipse Plus $C_{18}$ column (2.1 × 50 mm, 1.8 µm) at a temperature of 45 °C. The MS data were acquired over a range from 100–3000 m/z in positive mode. Auto MS/MS fragmentation was achieved with rising collision energy (35–50 keV over a gradient from 500–2000 m/z) with a frequency of 4 Hz for all ions over a threshold of 100. The UHPLC started with 90% $H_2O$ containing 0.1% acetic acid. The gradient began after 0.5 min to 100% acetonitrile (0.1% acetic acid) in 4 min. Two µL of a 1 mg/mL sample solution was injected to a flow of 0.8 mL/min. The HPLC was carried out on a Waters Breeze HPLC system equipped with a 1525 µ dual pump, a 2998 DAD detector, and a Rheodyne 7725i injection system and with a Waters Alliance HPLC system equipped with a Waters 2695 separation module and a Waters 996 PDA detector. A Macherey-Nagel Nucleodur $C_{18}$ Pyramid column (250 mm × 10 mm; 5 µm) and a Phenomenex Kinetex $C_{18}$ column (250 mm × 4.6 mm, 5 µm) were used for separation. For further information on NMR and MS data see supplementary information (SI).

### 2.3. MALDI-MS Imaging

Matrix-assisted laser desorption/ionization mass spectrometry imaging (MALDI-MSI) has become a fundamental analytical tool for analyzing substances in biological specimens. This method allows the correlation of spatial ion distribution with histological features. The MALDI-MSI experiments were performed at the Institute of Inorganic and Analytical Chemistry, Justus Liebig University Giessen, Germany. Matrix-assisted laser desorption/ionization mass spectrometry imaging (MALDI MSI) was used to map the distribution of the cytotoxin LatA. For this, the frozen specimens, two of *C. annae* and

one of *C. dianae*, were thawed and embedded in 5% (*w*/*v*) gelatin aqueous solution and refrozen at −80 °C for 60 min to form solid blocks. Afterwards, tissue sections of 20 µm thickness were sectioned using a cryomicrotome (HM 525 cryostat, Thermo Scientific, Dreieich, Germany) at −20 °C. The embedding material was removed carefully with a painting brush to prevent tissue distortion. Sections were thaw mounted on microscope glass slides and stored at −80 °C before analysis. The samples were brought to room temperature using a desiccator to avoid condensation of humidity. Optical microscopic images of the sections were captured before matrix application (Keyence VHX-5000 digital microscope (Keyence Deutschland GmbH, Neu-Isenburg, Germany).

A matrix preparation system (SMALDIPrep, TransMIT GmbH, Giessen, Germany) was used to spray 100 µL (10 µL/min) of the matrix solution (30 mg/mL of 2,5-dihydroxybenzoic acid in 50:50 (*v*/*v*) acetone:$H_2O$ (0.1% TFA) for low molecular weight compounds in positive ion mode), on top of the tissue sections. This provided uniform coating of the microcrystalline matrix material needed for high spatial resolution MALDI-MS imaging [134]. Before fixing the sample on the sample holder of the imaging source, homogeneity and crystal sizes were controlled after matrix application by microscopy.

The MALDI-MS imaging experiments were performed with a high spatial-resolution MS imaging ion source (AP-SMALDI10®, TransMIT GmbH, Giessen, Germany) operating at atmospheric pressure [135]. The minimum laser beam focus results in an ablation spot diameter of 5 µm [136–138]. However, for the experiment described here, the laser focus size was set to 10 µm. The samples were scanned by the movement of the x-, y-, and z-stages placed in front of the transfer capillary of the mass spectrometer. For desorption/ionization, a diode-pumped solid-state laser at 343 nm wavelength, operating at 100 Hz, was used. Generated ions were co-axially transferred to a high mass-resolution mass spectrometer (Q Exactive™, Thermo Fisher Scientific GmbH, Bremen, Germany, mass resolution, R = 140,000 at m/z 200). Mass spectra in the mass range of m/z 250–850 were generated, and the analyzer was operated in positive ion mode. For internal calibration of mass spectra, a ubiquitous signal of the MALDI matrix was used as a lock mass, providing a mass accuracy better than 2 ppm root mean square error. High-quality MS ion images were generated using the Mirion software package [139]. A narrow image bin width of $\Delta m/z = \pm 5$ ppm was used for image generation. The MS images were normalized to the highest signal intensity per image for each imaged analyte ion species. No additional data processing steps, such as smoothing, interpolation, or normalization to matrix signals, were employed. Red–green–blue (RGB) overlay images were generated for the selected analyte ion signals to demonstrate the distribution of LatA in *Chromodoris* cross-sections. The red ion signals were later edited to grey for better visibility.

### *2.4. Fluorescence Microscopy*

To investigate and visualize the activity of LatA, we administered the extracted compound to human embryogenic kidney cells (HEK293, obtained from Leibniz Institute, DSMZ GmBH, Braunschweig, Germany, reference number ACC 305) and analyzed effects under fluorescence microscopy. The HEK293 cells were cultivated in Dulbecco's modified Eagle's medium (DMEM), low glucose, pyruvate, supplemented with 100 units/mL penicillin, 100 µg/mL streptomycin, and 10% fetal calf serum. The HEK293 cells and all generated clones were maintained by ten-fold dilutions with fresh medium every 3–4 days in 10 cm dishes. All cells were cultured at 37 °C and 5% $CO_2$.

The HEK293 cells were seeded in a density of 12,500 cells per $cm^2$ on 18 mm glass coverslips in DMEM, supplemented with 100 units/mL penicillin, 100 µg/mL streptomycin, and 10% fetal calf serum, two days before the fluorescence imaging. Glass coverslips were coated using 50 µL of 0.1 mg/mL PDL solution for 30 min at 37 °C and were afterward washed three times with 50 µL PBS. After the cells attached to the coverslips, either only DMSO as control or 50 µM LatA (isolated and combined from several *Chromodoris* sea slug individuals) solved in DMSO, was added to the medium. When the cells of the DMSO-control group reached a density covering 75–90% of the glass coverslips, the experiment was stopped,

and cells were prepared for staining for further fluorescence imaging. To stain the cells, the medium was exchanged with 1 mL methanol free 4% paraformaldehyde/10% sucrose solution in PBS buffer and kept for 10 min at room temperature. This solution was exchanged with 1 mL 0.1% Triton in PBS buffer and was kept for 2 min at room temperature. Afterwards, the cells were washed two times with PBS buffer. Coverslips were incubated on parafilm, each with 50 µL Phalloidin-Atto 488-solution (1:500 in PBS/1% BSA) and Hoechst stain (500 ng/mL), in darkness, for 45 min at room temperature. Subsequently, coverslips were washed two times with PBS, one time with water, and were then mounted on a slide using Mowiol as a mounting medium. Fluorescence imaging was conducted with an Axiovert® 200 M microscope (Carl Zeiss Microscopy GmbH, Jena, Germany) equipped with a Colibri.2® LED system including a 365 nm LED, LD Achroplan 40×, NA 0.60 Korr. objective, AxioCamMR3® camera, and filter set 49 (Excitation: G 365, Beam Splitter: FT 395 Emission: BP 445/50). The system was operated with Axiovision® Rev. 4.8.

### *2.5. In Vivo Toxicity Assay*

Living specimens of *Chromodoris annae* (1) and *Chromodoris dianae* (2) were kept in glass aquaria with artificial seawater (Instant Ocean®, synthetic sea salt, added according to instructions), salinity around 33–34.5 PSU, relative density~1.025–1.026, at 26–28 °C, aerated via an oxygenation pump and air stone bubblers. Also, 12 living *Elysia viridis* specimens were kept in glass aquaria, with artificial seawater (Instant Ocean®, synthetic sea salt, added according to instructions), salinity around 36–37.5 PSU, relative density~1.0275–1.0286, at 17–19 °C, aerated via an oxygenation pump and air stone bubblers. The 12 *E. viridis* specimens were separated into two groups. As a control, six *E. viridis* were injected into the muscular foot with an isotonic solution (0.01 mL, 5% DMSO, SI Table S4), the other six *E. viridis*, one *C. annae* and two *C. dianae* were injected with an isotonic solution containing 75 µM LatA (0.01 mL, 5% DMSO). As only three live *Chromodoris* specimens were available, all of them were injected with LatA and there was no additional control *Chromodoris* group. Since all *Chromodoris* specimens survived the first experiment with the same amount of LatA applied as in the *E. viridis* specimens, the experiment was repeated a second time with a threefold and a third time with a fivefold increased amount of LatA to account for the size difference and thus, a possible difference in the concentration of LatA per body mass. Each injection was carried out with a fine dosage syringe (Omnifix®-F Luer Duo, Braun, 1 mL, 0.01 mL graduation, DIN EN ISO-Norm 7886-1) and a sterile, hypodermic Sterican® needle (25 G/0.5 × 26 mm, DIN EN ISO-Norm 7864). After injection, all animals were kept in separate groups and observed over several hours, or days, where appropriate. Symptoms, behavioral changes, including effects of a light stimulus, and deaths, if occurring, were documented.

### *2.6. Comparative Analysis of Heterobranchia Actin Genes*

Genomic DNA of 13 *Chromodoris* specimens (*C. annae* 4 sp., *C. dianae* 2 sp., *C. lochi* 2 sp., *C. strigata* 3 sp., *C. willani* 2 sp., material published by Undap et al. 2019) [18] and of one *Elysia viridis* specimen (by courtesy of G. Christa), (see Table 1) were provided. Based on available molluscan actin sequences from GenBank, NCBI [140], including several actin isoform sequences of *Aplysia californica* (Heterobranchia, Anaspidea), degenerated and subsequently, specific primers were designed for *Chromodoris* and the *Elysia* species. The following primers were designed for *Chromodoris* species resulting in sequences of a length of around ~ 885 bp: Forward "Act1F": 5′-CAG GGT GTT GGA GAA GAT CTG GCA TC-3′, and the reverse primer "Act1R": 5′-TAG AAG CAC TTC CTG TGG ACA ATG GA-3′ (Table 2). The following specific primers were designed for *Elysia viridis*, resulting in around 825 bp: Forward "F19_1": 5′-GGA GAA GAT CTG GCA TC-3′, and the reverse primer "R19_1": 5′-GAT CCA CAT CTG CTG G -3′. Amplification (PCR) of the targeted gene was performed by an initial step (98 °C for 30 s), followed by 32 touch-down cycles of denaturation (98 °C, 10 s), annealing (61 °C, 30 s) and extension (72 °C, 30 s), with a final extension step (72 °C, 2 min). The PCR products were separated using gel elec-

trophoresis (1% agarose, 110 V, 45 min) and stained with ethidium bromide (SI Figure S8). The fragments were isolated from the gel and purified using either the Zymoclean ™ Large Fragment DNA Recovery Kit (Zymo Research Europe GmbH, Freiburg, Germany) or the FastGene® Gel/PCR Extraction Kit (NIPPON Genetics Europe, Düren, Germany), according to the manufacturer's instructions. Purified PCR products were sent to Eurofins Genomics and sequenced by Sanger sequencing (Eurofins Genomics Germany GmbH, Ebersberg, Germany). Sequences covering the coding region had a length of 885 bp (*Chromodoris* species) and 827 bp (*Elysia* species). Consensus sequences were created for each species (for accession numbers, see Table 2). Additional transcriptomic cDNA sequences of cladobranch species (*Flabellina affinis*, *Embletonia pulchra*, *Armina tigrina*) were kindly provided by D. Karmeinski [141]. These species were selected to represent the sister group of the Doridina.

**Table 2.** Specimens used for designing primers of the putative actin gene fragment and accession numbers of the obtained consensus sequences of the five *Chromodoris* species and the *Elysia viridis* specimen.

| Species (Specimen Identifier) | Accession Number |
|---|---|
| *Chromodoris annae* (Chan16Sa-9, Chan16Sa-3, Chan16Bu-6, Chel16Sa-1) | OK074000 |
| *Chromodoris dianae* (Chdi16Sa-6, Chdi16Bu-6) | OK074001 |
| *Chromodoris lochi* (Chlo16Bu-1, Chlo16Bu-2) | OK074002 |
| *Chromodoris strigata* (Chmi16Bu-1, Chst16Sa-1, Chst17Ba-1) | OK074003 |
| *Chromodoris willani* (Chwi16Bu-1, Chwi16Bu-2) | OK074004 |
| *Elysia viridis* (gDNA by courtesy of G. Christa) | OK074005 |

The obtained Heterobranchia sequences (five *Chromodoris*, three *Cladobranchia*, one *Elysia* species and the most similar isoform of the three recognized *Aplysia* actin sequences (NM_001204640.1, *Aplysia californica* actin (LOC100533345), mRNA) [142], were aligned using the MUSCLE algorithm implemented in MEGA X version 10.0.5 [143]. A network analysis was performed using SplitsTree4 v4.16.2. [144], and ClustalX2.1 [145] was used for sequence identity and distance analyses. New actin sequences were blasted in NCBI Genbank and the closest hits were recorded. The new sequences are deposited in the NCBI GenBank database (accession numbers see Table 2). An *in silico* hybrid-model of a combination of the amplified and sequenced *Chromodoris* actin (286 aa) and subsequently added parts of an *Armina tigrina* actin sequence (89 aa), to approximate missing amino acids for a complete actin protein (375 aa), was created using the Phyre2 web portal for protein modelling, prediction and analysis (SI Figure S9) [146]. The model was displayed and colored in the program PyMOL Molecular Graphics System, Version 2.0 Schrödinger, LLC.

## 3. Results

### *3.1. Chemical Investigation of Chromodoris Nudibranchs and Cacospongia mycofijiensis*

The investigated extracts from the five closely related nudibranch species: *Chromodoris annae*, *C. dianae*, *C. lochi*, *C. strigata* and *C. willani* (see Figure 3), as well as one of the associated sponge prey, *Cacospongia mycofijiensis* (Thorectidae, Porifera), and the mucus trails contained a shared metabolite with protonated ion fragments and adducts typical for the 2-thiazolidinone macrolide LatA (*m/z* 386 $[M + H-2H_2O]^+$, 404 $[M + H-H_2O]^+$, 422 $[M + H]^+$ and 444 $[M + Na]^+$, SI Figures S1–S4). The metabolite was isolated by HPLC and conclusively identified as LatA (400 µg/specimen) by further 1D and 2D NMR spectroscopy (Figures 4, S5 and S6, Tables S1 and S2), optical rotation measurements, and comparison to the literature [38,46,48,112,147,148]. The HPLC-MS analysis revealed espe-

cially high concentrations of LatA in the extracts of the dissected mantle rim containing the MDFs, in comparison to the body (SI Figure S2). LatA was also present in small amounts in the mucus trail, as well as in the mucus removed directly from the notum (SI Figure S1). We observed members of several *Chromodoris* species feeding on *C. mycofijiensis* in the field (SI Figure S7), a finding not reported before. Isolation of LatA from the collected nudibranch and respective sponge food (SI Figure S1), further supports this dietary relationship at least in North Sulawesi. However, not all specimens were found invariably living and feeding on *C. mycofijiensis*. For example, we also found *Chromodoris* nudibranchs on sponges belonging to the Thorectinae subfamily and the Petrosiidae family (SI Figure S7). These findings may support the hypothesis that *Chromodoris* sea slugs have less specialized alimentary habits than previously thought [11,149].

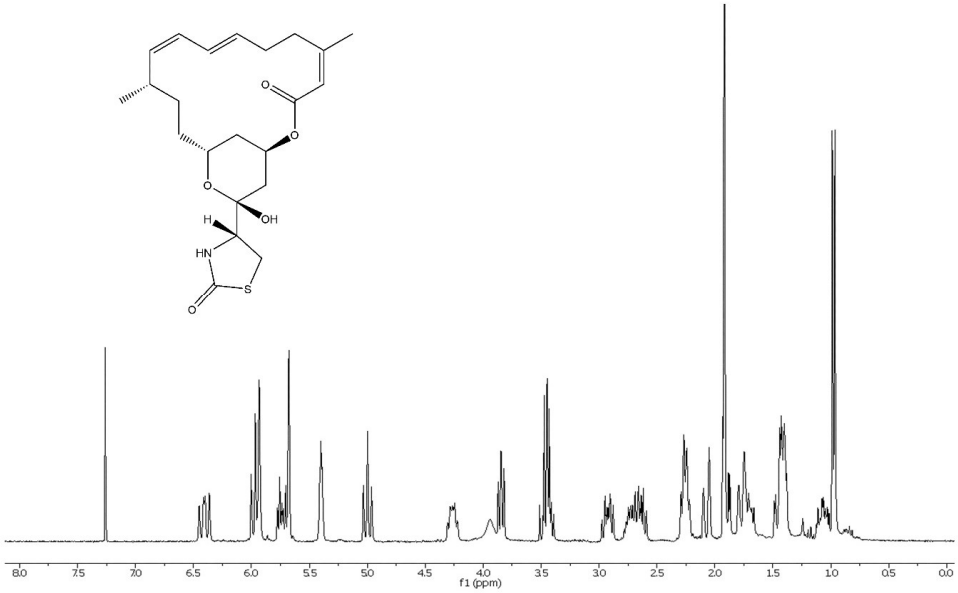


**Figure 4.** $^{1}$H-NMR spectrum of latrunculin A in $CDCl_3$.

### *3.2. MALDI-MS Imaging*

Our MALDI-MSI analyses revealed that LatA is stored in the mantle tissue, especially in vacuoles of the mantle dermal formations (MDFs) (Figures 5 and S4). Additionally, LatA was found in mucus glands and the mucus (Figure 5(A2,B2)). Especially the investigated *C. dianae* exhibited a copious amount of stained mucus around the body (Figure 5(B2)), whereas in *C. annae*, it concentrated between mantle rim and foot. Remaining traces of LatA were also found in the pharynx and the marginal area of the digestive gland of *C. annae* (Figure 5(A2)), further supporting a dietary origin of LatA.

### *3.3. Fluorescence Microscopy*

Incubation of HEK-293 cells with 50 µM LatA, isolated and pooled from several *Chromodoris* specimens, led to collapsed, deformed and rounded-up cells within the first 24 h, due to the destruction of the filamentous actin (Figure 6B). The process was also confirmed after 44 h (Figure 6C). In contrast, the control did not lead to any deformation of the kidney cells within the 44 h of measurement (Figure 6A). This indicates that LatA is stored active and unaltered in the body of *Chromodoris* nudibranchs.

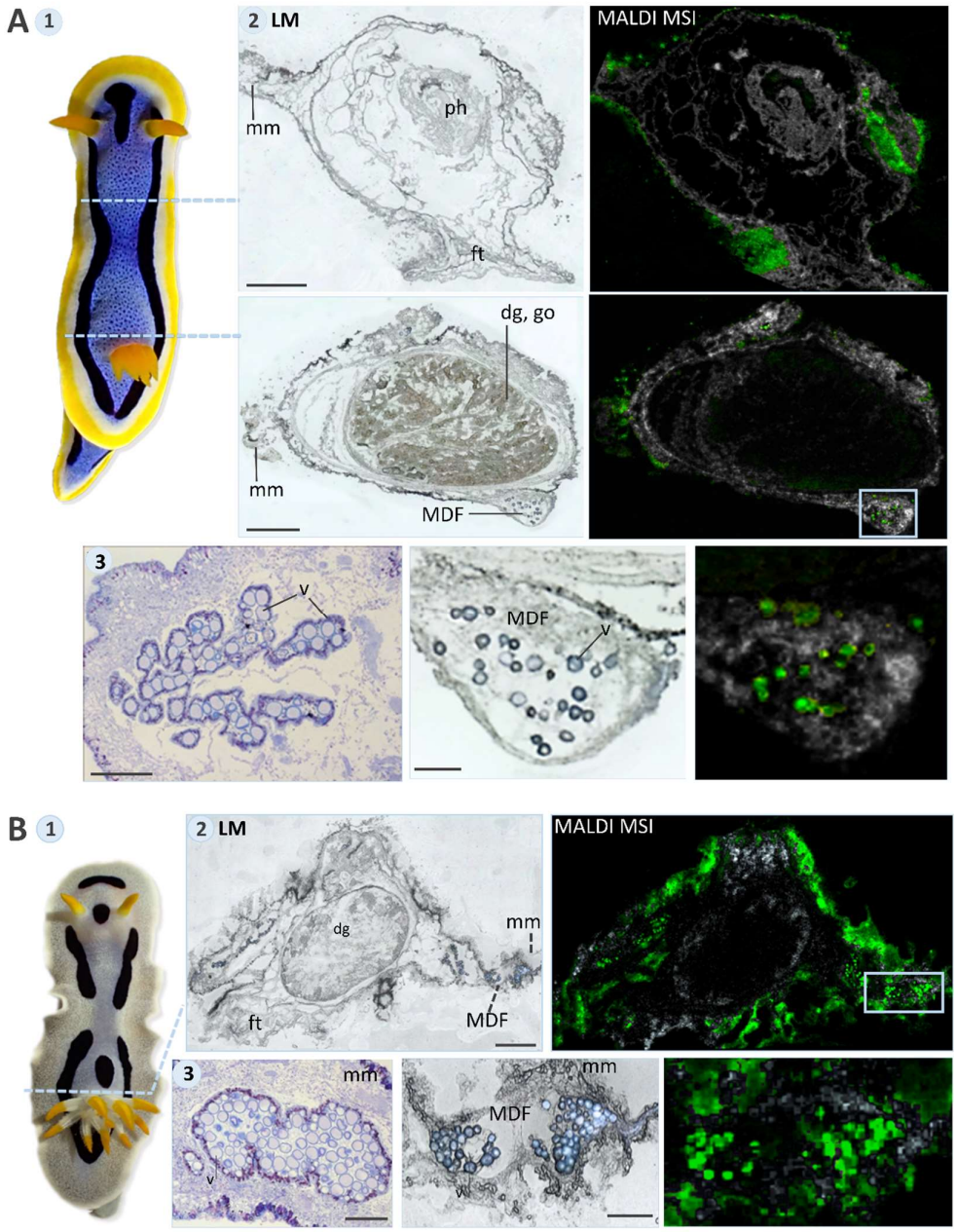


**Figure 5.** Comparison of optical and MALDI mass spectrometry images, revealing the distribution of LatA (green) in (**A**) *Chromodoris annae* and (**B**) *Chromodoris dianae*. (**A1**) Dorsal overview of a *Chromodoris annae* specimen. (**A2**) Overview of the anterior and middle cross-sections (20 µm, dotted lines) of *C. annae* by light microscopy and MALDI MSI, showing the distribution of LatA (*m/z* 444.1813 $[M + Na]^+$, 10 µm/pixel) in green. Square indicating MDF, which is shown as a close-up in: (**A3**) Close-up view of a *C. annae* MDF, from left to right: histological section from another specimen, optical and MALDI image. (**B1**) Dorsal overview of a *Chromodoris dianae* specimen. (**B2**) Overview of the posterior cross-section (20 µm, dotted line) of *C. dianae* by light microscopy and MALDI MSI, showing the distribution of LatA (*m/z* 444.1813 $[M + Na]^+$, 10 µm/pixel) in green. Square indicating MDF, which is shown as close-up in: (**B3**) Close-up view of a *C. dianae* MDF, from left to right: histological section (from another specimen), optical and MALDI image. Abbreviations: **dg**, digestive gland; **ft**, foot; **gc**, gill circle; **go**, gonads; **LM**, light microscopy; **MALDI MSI**, matrix-assisted laser desorption/ionization mass spectrometry imaging; **MDF**, mantle dermal formation; **mm**, mantle margin; **ph**, pharynx; **v**, vacuole. Scale bars: **A/B2** = 1000 µm; **A/B3** = 200 µm.

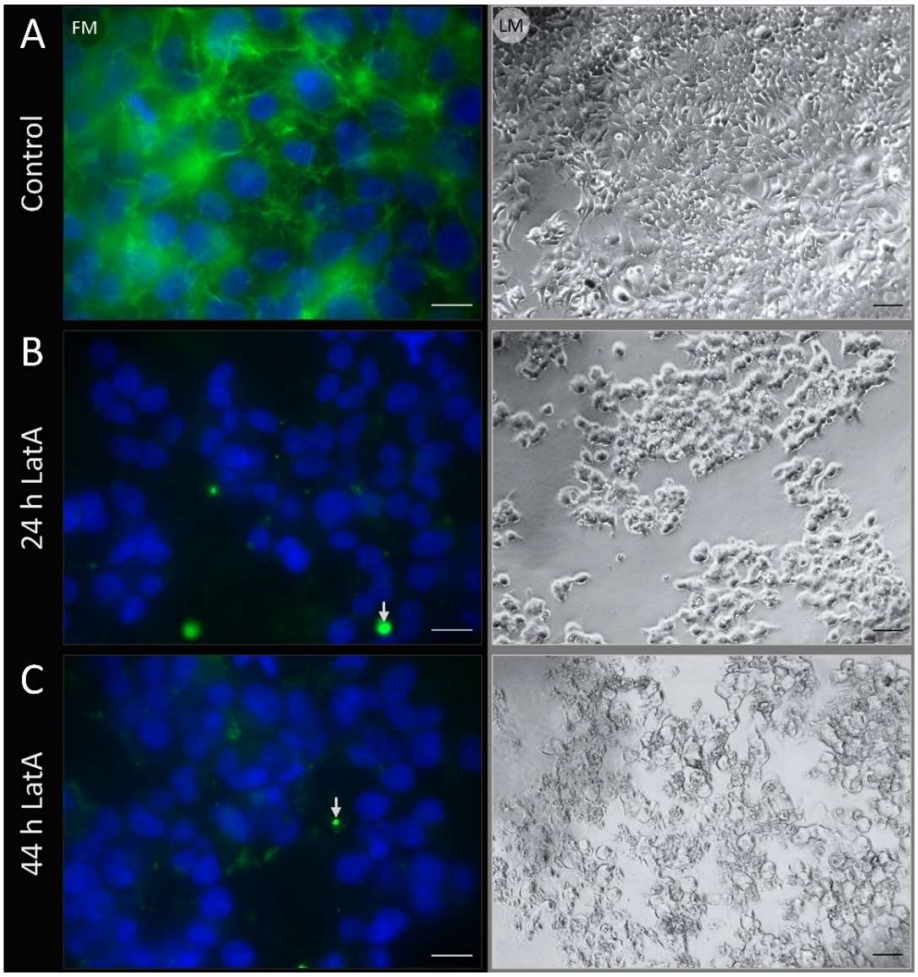


**Figure 6.** Cytoskeletal visualization of HEK-293 cells using fluorescent microscopy (**FM**, left) with Phalloidin staining filamentous actin (green), and Hoechst staining DNA (blue), in comparison to light microscopy images (**LM**, right column). Cells were incubated in DMEM medium (**A**) without LatA (control, 44 h), (**B**) with 50 µM LatA, isolated from *Chromodoris* nudibranchs for 24 h, (**C**) with 50 µM LatA for 44 h. Arrows mark condensed actin. Scale bars: **FM** = 20 µm; **LM** = 50 µm.

### *3.4. In Vivo Toxicity Assay*

All specimens (*Chromodoris* and *Elysia*) showed defensive responses during the insertion of the needle, by exposing the mantle area with the MDFs (*Chromodoris*) or the parapodia (*Elysia*), contracting the foot and the rest of the body. This behavior likely deflects attacks toward the defensive tissue and away from the vulnerable body parts containing the viscera.

All six control group *Elysia viridis* specimens (isotonic solution only), survived the injections, returned to their provided food source *Codium fragile* and continued feeding. In contrast, the six *Elysia* specimens injected with the isotonic solution containing 75 µM LatA died. They showed the same defensive response as the control group during the needle insertion. Yet afterwards, they did not return to 'normal' behavior. Instead, their movement was highly constrained within 1–3 min and they could not return to their food source. These six *E. viridis* specimens were observed throughout the day, and they were declared dead at the end of the day when no recovery, no general movement, and no response to touch or light stimuli could be observed.

All three *Chromodoris* specimens injected with LatA, survived all three experiments. No LatA intoxication or further defensive responses were observed for the *Chromodoris* nudibranchs, neither during the first experiment, where the same amount of LatA was used as in the *Elysia* specimens, nor during the second and third experiments, where the amount

of LatA was increased threefold and fivefold, respectively, to account for the difference in size. When an additional light source was switched on, the animals exhibited defense and escape behavior, by either contracting their body or quickly moving away from the light, as was also observed before the toxicity experiment.

### *3.5. Comparative Analysis of Heterobranchia Actin Genes*

We assumed that the protein target of LatA, i.e., actin is mutated in *Chromodoris* nudibranchs, and this way, they may be insensitive to the toxin. Thus, sequences encoding for actin were evaluated in *Chromodoris* and compared to those in other related taxa. For comparison with the taxon Doridina, to which the genus *Chromodoris* is assigned, three species of the sister taxon Cladobranchia were selected from published transcriptomes [141]. These three species mainly protect themselves by incorporation of cnidocysts (*Flabellina affinis*), or other secondary metabolites, but not LatA (*Armina tigrina*, *Embletonia pulchra*) [150]. *Elysia viridis* (sequenced new) and *Aplysia californica* (actin sequences extracted from GenBank, NCBI, [140]) belong to further different heterobranch taxa, the Sacoglossa and Anaspidea, respectively. Members of both taxa feed on different algae and obtain their defensive compounds from these algae. The newly obtained sequences covering the coding region had a length of 885 bp (*Chromodoris* species) and 827 bp (*Elysia* species). Aligning these sequences together with the other extracted heterobranch sequences resulted in an alignment with 808 nucleotides and 269 amino acid positions in length. Our comparative studies on the 13 heterobranch species revealed a new actin isoform sequence in *Chromodoris* species that differed considerably to that of the other heterobranch actin sequences, but only by few mutations within the genus *Chromodoris* (Figure 7, Table 3). According to the reported mutations in quite different lifeforms, including *Picea*, *Saccharomyces*, and *Homo sapiens*, which cause LatA resistance (see SI Table S3 and references cited therein), we searched for similar mutations in the heterobranch alignment. In this respect it is important to note that amino acids differ in their physico-chemical properties, i.e., they are characterized as polar acidic (i.e., can donate a proton), polar basic (i.e., can accept a proton), polar neutral (uncharged) and nonpolar, affecting the structure of the respective protein and its biological function. The here identified *Chromodoris* actin gene sequences show two crucial point mutations, g.560A > G (p.D187G) and g.617G > C (p.R206T), that lead to amino acid substitutions with changes in properties (Figure 7). The acidic aspartic acid D187 and the basic arginine R206 usually form a hydrogen and ionic bond (a salt-bridge), essential for the stabilization of the tertiary structure of actin and binding of latrunculins (see Figure 8) [55,101,151]. Their substitutions to the nonpolar amino acid glycine D187G and neutral threonine R206T disable the formation of this salt-bridge, which results in alteration of the 3D actin structure. This in turn could lead to a repulsion of LatA and thus, to resistance.

Several further differences in the latrunculin-binding region can be detected in all investigated *Chromodoris* nudibranchs, of which most represent substitutions of amino acids with similar chemical properties, such as lysine (polar basic) to arginine (polar basic), serine (polar neutral) to asparagine (polar neutral), or threonine (polar neutral) to serine (polar neutral). However, the flanking amino acids threonine T186 and arginine R210 (Figure 7), which directly bind to latrunculins, are conserved in all investigated heterobranchs, including *Chromodoris*. Distance analyses (percent identity matrices) and network analyses of the Heterobranchia revealed near-identical actin sequences with ≥98% DNA sequence identity (100% identity on AS level) (Figure 9, Table 3) between the five *Chromodoris* species, but only ≥68% identity at the DNA level (≥75% identity at the amino acid level) with other heterobranch actin sequences. Cladobranchia actin sequences showed higher similarity to the anaspid *Aplysia californica* and sacoglossan *Elysia viridis* (≥82% identity at the DNA level; ≥92% identity at the amino acid level) than to the *Chromodoris* actin isoform sequences (Figure 9, Table 3).

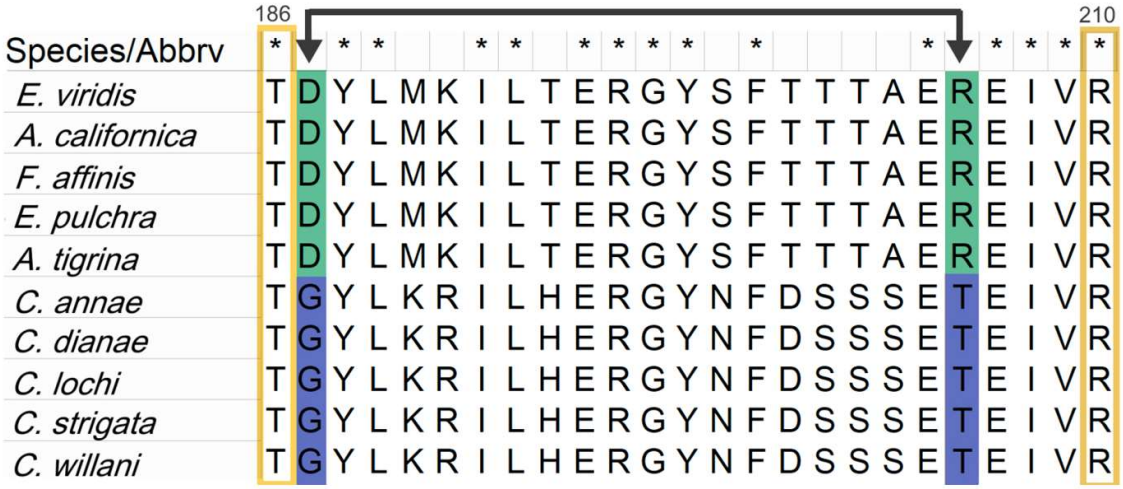


**Figure 7.** Multiple consensus amino acid sequence alignments of the latrunculin-binding region of heterobranch actins. Threonine T186 and arginine R210, directly interacting with latrunculins, are framed with yellow rectangles. Aspartic acid D187 and arginine R206 forming a salt bridge (indicated by arrows) are highlighted in green. The substitutions D187G and R206T are highlighted in blue. Highly conserved amino acids are marked with an asterisk.

**Table 3.** Percent identity matrices of heterobranch actin sequences. (1) Identity matrix based on 808 nucleotide positions. (2) Identity matrix based on 269 amino acid positions. Values > 80% are shown in bold.

| (1) | *C. annae* | *C. dianae* | *C. strigata* | *C. lochi* | *C. willani* | *F. affinis* | *A. tigrina* | *E. pulchra* | *A. californica* | *E. viridis* |
|---|---|---|---|---|---|---|---|---|---|---|
| *C. annae* | | **99** | **99** | **99** | **99** | 70 | 69 | 70 | 69 | 69 |
| *C. dianae* | **99** | | **98** | **99** | **99** | 70 | 69 | 70 | 69 | 69 |
| *C. strigata* | **99** | **98** | | **98** | **99** | 70 | 69 | 70 | 70 | 69 |
| *C. lochi* | **99** | **99** | **98** | | **99** | 69 | 68 | 70 | 69 | 69 |
| *C. willani* | **99** | **99** | **99** | **99** | | 69 | 69 | 70 | 69 | 69 |
| *F. affinis* | 70 | 70 | 70 | 69 | 69 | | **82** | **87** | **85** | **87** |
| *A. tigrina* | 69 | 69 | 69 | 68 | 69 | **82** | | **87** | **87** | **85** |
| *E. pulchra* | 70 | 70 | 70 | 70 | 70 | **87** | **87** | | **88** | **89** |
| *A. californica* | 69 | 69 | 70 | 69 | 69 | **85** | **87** | **88** | | **91** |
| *E. viridis* | 69 | 69 | 69 | 69 | 69 | **87** | **85** | **89** | **91** | |
| **(2)** | *C. annae* | *C. dianae* | *C. strigata* | *C. lochi* | *C. willani* | *F. affinis* | *A. tigrina* | *E. pulchra* | *A. californica* | *E. viridis* |
| *C. annae* | | **99** | **99** | **99** | **100** | 76 | 77 | 77 | 76 | 77 |
| *C. dianae* | **99** | | **99** | **100** | **100** | 76 | 77 | 76 | 75 | 77 |
| *C. strigata* | **99** | **99** | | **99** | **100** | 76 | 77 | 77 | 76 | 77 |
| *C. lochi* | **99** | **100** | **99** | | **100** | 76 | 77 | 76 | 75 | 77 |
| *C. willani* | **100** | **100** | **100** | **100** | | 76 | 77 | 77 | 76 | 77 |
| *F. affinis* | 76 | 76 | 76 | 76 | 76 | | **92** | **93** | **93** | **93** |
| *A. tigrina* | 77 | 77 | 77 | 77 | 77 | **92** | | **95** | **95** | **96** |
| *E. pulchra* | 77 | 76 | 77 | 76 | 77 | **93** | **95** | | **97** | **97** |
| *A. californica* | 76 | 75 | 76 | 75 | 76 | **93** | **95** | **97** | | **96** |
| *E. viridis* | 77 | 77 | 77 | 77 | 77 | **93** | **96** | **97** | **96** | |

Overall, the newly obtained *Elysia* actin sequence and the *Aplysia* actin sequence, obtained from GenBank (NCBI) [140], showed higher sequence identity to other Gastropoda sequences available in the GenBank database, than to the newly obtained isoform from *Chromodoris* sea slugs (SI Tables S5–S10), which instead matched highest with lancelet actins, *Branchiostoma floridae* $\leq$ 79.5% amino acid identity, and predicted squirrel actins, *Urocitellus parryii* $\leq$ 72.4% DNA sequence identity. The obtained *Elysia* actin sequence showed high sequence identity with actins of the Heterobranchia *Plakobranchus ocellatus* van Hasselt, 1824, *Elysia marginata* (Pease, 1871) (98.5% amino acid sequence identity each), *Elysia chlorotica* Gould, 1870, and *Biomphalaria pfeifferi* (Krauss, 1848) (97.8% amino acid sequence identity each), whereas the *Aplysia* actin matched highest with another *Aplysia* actin isoform (98.1% amino acid sequence identity) and the gastropods *Littorina littorea* (Linnaeus, 1758) and *Pomacea canaliculata* (Lamarck, 1819) (97.8% amino acid sequence

identity each). This shows high conservation of the *Elysia* and *Aplysia* actin isoform amino acid sequences (>97%) even to more distantly related families, whereas the newly obtained *Chromodoris* actin isoform sequences are more divergent, with the highest amino acid sequence identity to other gastropods found for actin isoforms of *Haliotis iris* Gmelin, 1791 (>78%).

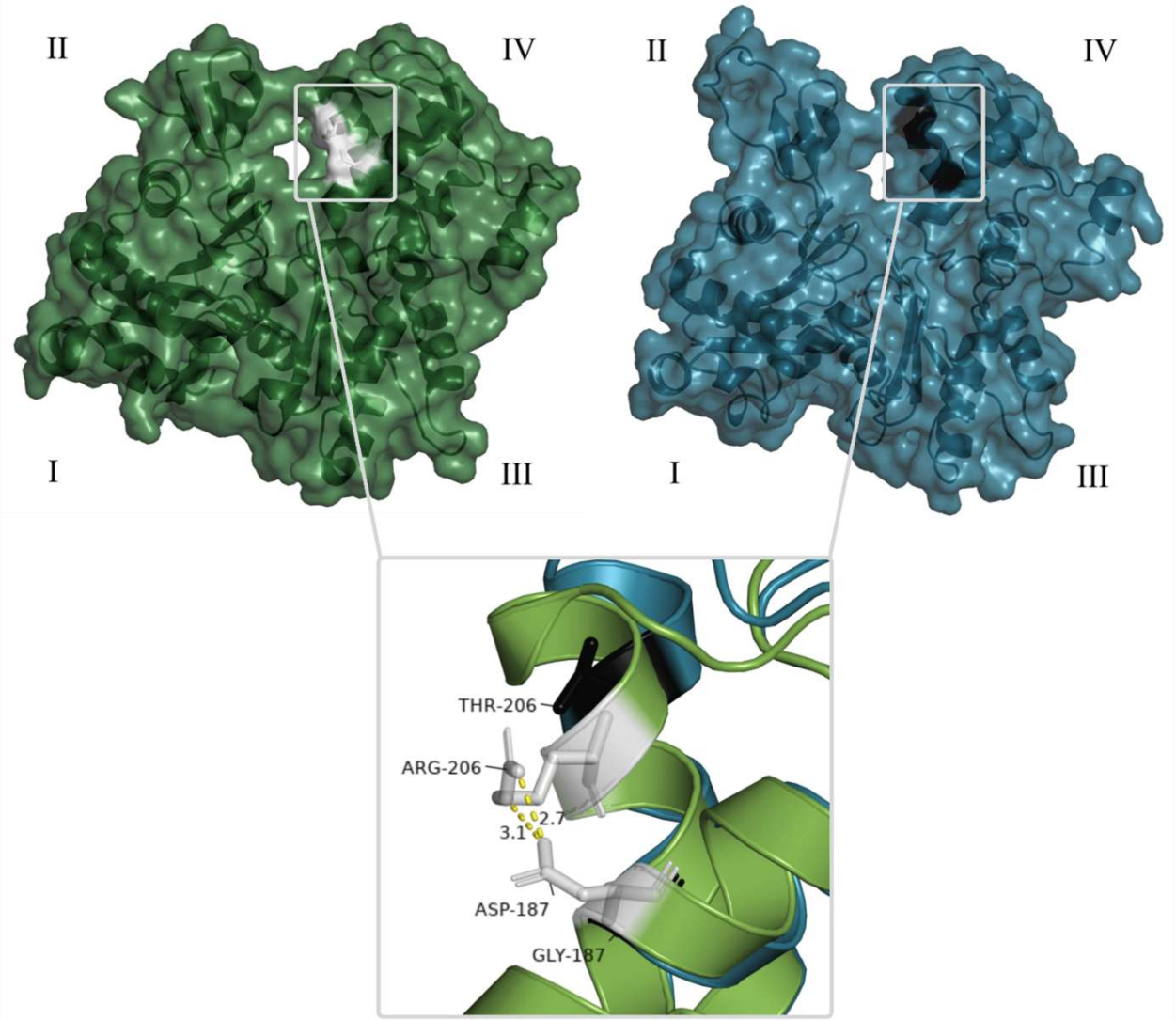


**Figure 8.** Overall comparison (upper left and right) and close-up comparison (lower middle) of a model of native G-actin (green, upper left, PDB: 3HBT, 375 aa) and an *in silico* hybrid-model of a combination of the amplified and sequenced *Chromodoris* actin (286 aa) and subsequently added parts of an *Armina tigrina* actin sequence (89 aa), to approximate missing amino acids (blue, upper right, 375 aa). Native aspartic acid D187 (ASP, acidic) and arginine R206 (ARG, basic), shown in white, form a salt bridge (yellow lines, 3.1 and 2.7 Å), whereas the substitutions glycine G187 (GLY, nonpolar) and threonine T206 (THR, neutral), shown in black, present in *Chromodoris* actin, do not interact. Both substitutions are adjacent to the nucleotide binding cleft and are part of the latrunculin-binding region.

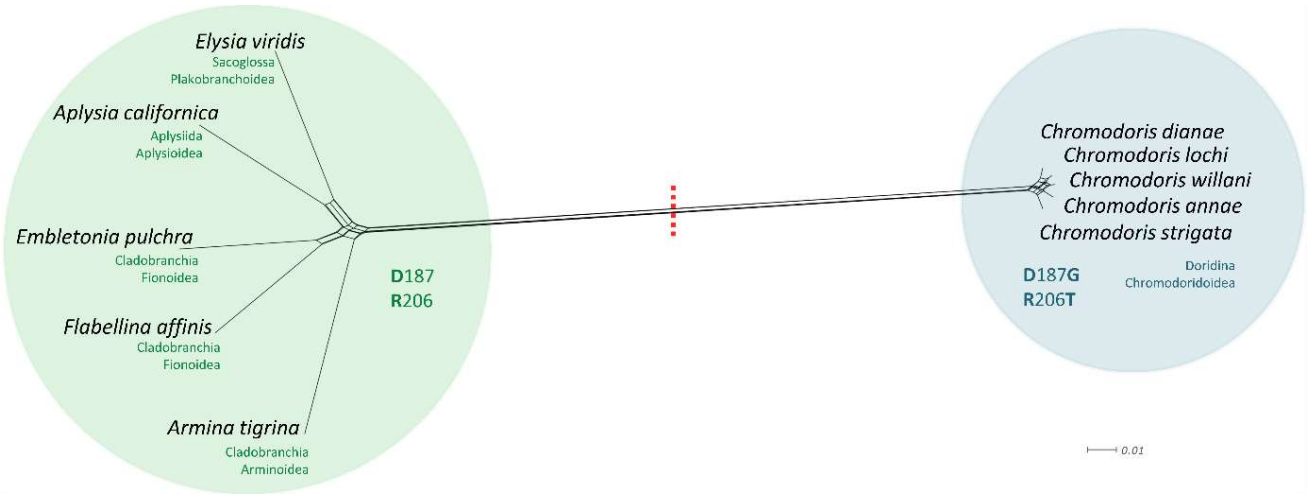


**Figure 9.** Unrooted phylogenetic split network of heterobranch actins, showing two distinct actin groups. Separation is indicated by a dotted red line. The network is based on the core nucleotide coding region (808 bp) of combined genomic gDNA (*Chromodoris* and *Elysia*) and transcriptomic cDNA (*Armina*, *Embletonia*, and *Flabellina*) actin sequences. The *Aplysia californica* actin sequence was obtained from GenBank. Sequences were aligned using the MUSCLE algorithm in MEGA X version 10.0.5. The split network was generated using SplitsTree4 v4.16.2. and the NeighborNet method. The scale bar indicates 0.01 substitutions/site.

## 4. Discussion

All members of the five investigated *Chromodoris* species were found to sequester and store LatA as a major metabolite. Until now, the incorporation of latrunculins has been reported for Australian *Chromodoris annae*, *C. elisabethina*, *C. kuiteri*, *C. lochi* and *C. magnifica* [11,15,35,37,39], South and East African *C. hamiltoni* [36,40], as well as for *C. quadricolor* [41,42], and *C. africana* from the Red Sea [43]. We therefore confirm here the presence of LatA for members of *C. annae* and *C. lochi* from Indonesia, and describe the compound new to *C. dianae*, *C. strigata* and *C. willani*.

LatA was also isolated from one of the respective sponge foods, *C. mycofijiensis* (SI Figures S1 and S7), which supports a dietary origin of LatA and additionally broadens the known food range of *Chromodoris* species to this special sponge species. Feeding traces on *C. mycofijiensis* (SI Figure S7), as well as remnants of LatA in the pharynx and digestive tract (Figure 5) further confirm the origin of this toxin from the food. Our studies show that LatA was not biotransformed by *Chromodoris* nudibranchs, but instead stored actively within the mantle rim, mucus glands and MDFs and thus retained its cytotoxic activity. This was experimentally shown in HEK-293 cells (Figure 6), which died after they were exposed to our extracted LatA. This is in contrast to other members of Heterobranchia, even members of the Chromodorididae (*Felimare, Glossodoris)*, where biotransformation as a detoxification mechanism has been proposed [3,22,123,152–157]. However, these sea slugs do not accumulate latrunculins in compartments, but other sequestered compounds from their diet, such as the sesterterpenoid scalaradial, which is transformed into related molecules, in particular 6-keto or 12-keto derivatives [3,22,123,152–157]. The MALDI-MSI was used on cross-sections of *C. annae* and *C. dianae* (Figure 5) to visualize the long-proposed hypothesis that MDFs of the mantle tissue act as important storage compartments for toxic compounds and potent defensive toxin packages [1,111,120–126,158–160]. Hamilton et al. applied the same technique to a different *Chromodoris* species, *C. kuiteri*, with similar results [39]. *Chromodoris* nudibranchs compartmentalize LatA, a mechanism that is commonly used to prevent autotoxicity, indicating that the initial role of these vacuoles and accumulation structures might have been excretory or auto-protection and evolved later into a defensive organelle [129]. A similar compartmentalization was also

described in a prey sponge *N. magnifica* in the Red Sea, storing high concentrations of LatB within membrane-bound, actin-free vacuoles in archeocytes [54]. Future studies might reveal that compartmentalization and storage of latrunculins in actin-free vacuoles is a common mechanism to cope with these toxic substances among organisms producing or sequestering them.

Furthermore, we found that LatA is present in the epidermis and mucus glands, as well as in the mucus from the notum. This might indicate a continuous excretion of the compound together with the mucus and thus, act as an additional repellent to putative predators, or as an antifouling agent. We also found a small amount of LatA in the mucus trail (SI Figure S1), which could serve as a chemical cue for additional purposes, such as chemical communication [11,30,161]. LatA has low solubility in water (~0.02 mg/mL), allowing for short-range chemical communication in aqueous environments through taste. The use of LatA as a semiochemical in the mucus trail could simultaneously inform and attract mating partners, while deterring predators from trying to follow the trail. For gastropods, the production of mucus is vital, but costly, and several behavioral adaptations, such as trail following, have evolved to compensate for energy losses [21,28,162]. However, leaving a trail poses a risk, as it reveals the position not only to mating partners, but also to predators. It has been shown that gastropod conspecifics and predators alike can pick up various cues, allowing them to determine the polarity (i.e., direction) of the trail and follow it to the mucus-producing organism [21,28]. Many, but not all, *Chromodoris* nudibranchs are known to display bright and contrasting coloration where MDFs are distributed in the mantle tissue, thus acting as visual signals, such as aposematic coloration and the use of mimicry, to advertise their toxicity [11,18–20,125,128,129,160,163]. Addition of LatA to the mucus would deter putative predators with poor vision or when visibility is not guaranteed, therefore playing an important role in enhancing warning signals.

Every eukaryotic cell depends on the many structures and functions provided by the evolutionary ancient protein actin or its variant isoactins [86,88,89,91–97,164–168]. With our experiments, we were able to confirm that LatA targets the actin cytoskeleton. Therefore, LatA is a highly effective defensive compound against any eukaryotic predator. This potency was recently shown experimentally by Winters et al. who classified LatA as a highly toxic and highly unpalatable toxin (Class I and II) to a number of potential model predators [15]. However, this also requires the resistance of the user storing the toxin, in this case, *Chromodoris* nudibranchs, to its cytotoxicity.

This putative resistance against the toxic LatA, was confirmed here in *in vivo* experiments with direct administration of LatA into living slugs. As was expected, the unrelated sacoglossan heterobranch *Elysia viridis* showed 100% mortality, which is in accordance with other toxicity assays where LatA also caused 100% mortality in mosquitofish and brine shrimp [11,169]. In contrast, the *Chromodoris* specimens survived all the experiments and returned to normal behavior shortly after the injection.

The injection evoked first some behavioral response within all specimens (control as well as with LatA injected), similar to the descriptions of defensive behavior of other nudibranchs [170–172]. Survival of *Chromodoris* specimens shows that the slugs are immune to the toxic substance and that the slugs' actin formation is not impaired.

Considering LatA's mode of action [55,60,79], known established mechanisms for the evolution of toxin resistance [107–109,173,174], and studies reporting individual cases of resistance to LatA [51,52,55,60,99–105], prompted us to sequence and compare several heterobranch actin genes to find a possible molecular resistance mechanism in *Chromodoris* nudibranchs. This is the first time that any underlying molecular resistance mechanism in heterobranch sea slugs toward sequestered toxic molecules has been investigated. We identified a novel actin isoform in all examined *Chromodoris* species containing two crucial amino acid substitutions at the 'nucleotide binding' cleft, the binding site of LatA (Figure 7). In a previous study, a mutation of D187 has experimentally been shown to inhibit latrunculin binding in Norway spruce (see SI, Table S3) [101]. So far, latrunculin-resistant actins have been found in yeast (*Saccharomyces*), Norway spruce (*Picea abies*), and human patients

with Baraitser-Winter syndrome, in which a strengthened G-actin monomer–monomer interaction, increased F-actin content and stability, and an overall influence on the composition of actins in the F-actin pool and dynamics of polymerisation is suggested. These changed properties are considered responsible for increased resistance against the depolymerizing activity of LatA [100,102,103,151,175]. Based on these reports and our results, we infer that the substitutions D187G and R206T of the 'nucleotide binding' cleft lead to target-site modifications, interfering with LatA binding, hence causing insensitivity to LatA. The D187G/R206T isoactin could enable *Chromodoris* nudibranchs to sequester LatA from *C. mycofijiensis* (and other sources) and compartmentalize it in their mantle tissue for defense, without having to suffer from its cytotoxicity. Nevertheless, these results are only a first step towards a better understanding of toxin resistance in nudibranchs and do not exclude other possible resistance mechanisms that could be exploited in synergy. Additional studies regarding heterobranch actins and their expression, as well as a full characterization of the novel *Chromodoris* actin isoform, its physico-chemical properties and the affinity of its binding sites, are needed to further investigate and verify this hypothesis.

In most eukaryotes, actin proteins consist of multiple isoforms with overlapping but non-redundant functions, encoded by structurally related genes that evolved by duplication and divergence from a common ancestral gene [89,91,97,164,166,168]. Convergent toxin resistance, driven by gene duplications and substitutions, is commonly observed among organisms in chemically defended, antagonistic predator-prey relationships [176–178]. Duplications of the actin gene with followed diversification are also common and known from freshwater and marine gastropods [142,179–184]. The increased divergence of the new *Chromodoris* actin isoform to the other heterobranch actins by $\geq$23% at the amino acid level (Table 3, Figure 7) could be attributable to duplication events and further speciation in chromodorid nudibranchs. In this case, mutations of the novel isoactin, leading to resistance against latrunculins, would provide an inheritable evolutionary advantage to *Chromodoris* nudibranchs. This additional isoactin would enable the slugs to forage on a specific diet that contains latrunculins, while maintaining the functionality of the essential native actin.

Still, little is known about the diversity, classification, expression and molecular evolution of actin isoforms in marine molluscs and this is the first study to investigate them for a member of the Heterobranchia, which are known for a long time to sequester and store actin-binding, cytotoxic metabolites. For example, the dorid sea slug *Hexabranchus sanguineus* (Rüppell & Leuckart, 1830) accumulates kabiramides and ulapualides [23,72,82,98,185–188], and the anaspidean *Aplysia kurodai* Baba, 1937 sequesters the toxic macrolide aplyronine A [72,82,189–192]. Kabiramides, ulapualides and aplyronine A have a similar mode of action as latrunculins; however, they bind to the hydrophobic 'target binding' cleft between subdomains I and III of G-actin monomers, like all other actin-depolymerizing macrolides, and unlike latrunculins to the 'nucleotide binding' cleft, between subdomains II and IV [55,60,79,90,193,194]. Another intriguing question is how members of the genus *Gymnodoris* (Doridina) developed toxin resistance, given that they are known to be fierce predators of other sea slugs, including chromodorids [21]. Future studies may reveal additional actin isoforms, which would allow a more detailed analysis of the evolution of actin proteins in this so far neglected group and their importance in toxin resistance and chemical defense.

## 5. Conclusions

We found that nudibranchs of the genus *Chromodoris,* collected in North Sulawesi, Indonesia, sequester the highly cytotoxic macrolide LatA from one of their food sources, which in this study was observed to be *Cacospongia mycofijiensis*. They accumulate LatA untransformed in their mantle tissue and mucus glands. In particular, LatA was compartmentalized in high amounts in the vacuoles of MDFs, emphasizing their importance as a subcellular toxin repository. Furthermore, LatA was secreted with the mucus, possibly as a semiochemical to attract mating partners and deter predators. LatA's cytotoxicity directly

results from its binding to one of the essential eukaryotic proteins, G-actin monomers, prohibiting their polymerization and severing the F-actin network, ultimately resulting in the collapse and death of the cell. However, *in vivo* experiments with direct administration of LatA led to a mortality of 100% in *Elysia viridis* sea slugs and 0% mortality in *Chromodoris* nudibranchs. We amplified, sequenced, and described a novel actin isoform from all investigated *Chromodoris* species, carrying crucial amino acid substitutions at the 'nucleotide binding' cleft of actin, the binding site of LatA. Especially the amino acid substitutions D187G and R206T, which usually form an important salt-bridge, have been identified as possible underlying genetic mechanisms resulting in LatA resistance. This is the first study investigating a molecular mechanism of resistance in a group of heterobranch sea slugs and improving our understanding of a possible gene-based resistance mechanism in *Chromodoris* sea slugs against the cytotoxin LatA. We hypothesize, that the resistance to LatA is caused by a novel D187G/R206T isoactin, which would enable *Chromodoris* nudibranchs to sequester the toxin from their prey *C. mycofijiensis* (among others). Furthermore, this would allow them to store LatA for a longer period in the mantle tissue and use it for their defense, without suffering from its cytotoxicity.

Additionally, the bright or contrasting coloration of the mantle tissue where MDFs are distributed would draw the attention of predators to this chemically well-defended area [125,128,129,160,163].

We hope our work emphasizes the potential of toxin and resistance research in heterobranch sea slugs, by combining insights from a chemical, molecular, ecological, and cell biological perspective. Many questions remain to be resolved and we hope to inspire future studies investigating marine gastropod isoactins, their evolution, expression, physico-chemical properties and possible implications for cytotoxin resistances.

**Supplementary Materials:** The following supporting information can be downloaded at: https://www.mdpi.com/article/10.3390/d15020304/s1.

**Author Contributions:** Conceptualization, C.H., G.M.K. and H.W.; methodology, C.H., D.R.B., S.A., S.K. and T.F.S.; formal analysis, C.H.; investigation, C.H.; resources, C.H., N.I.J.U., A.P., D.R.B., S.A., R.B., F.K., T.F.S., H.W. and G.M.K.; data curation, C.H.; writing—original draft preparation, C.H.; writing—review and editing, C.H., H.W. and G.M.K.; supervision, G.M.K. and H.W.; funding acquisition, G.M.K., T.F.S. and H.W. All authors have read and agreed to the published version of the manuscript.

**Funding:** We thank the German Federal Ministry of Education and Research (BMBF) for funding the project "INDOBIO Indonesian Opisthobranchs and associated microorganisms—From biodiversity to drug lead discovery" with Grant Number 16GW0117K (GK and TFS) and 16GW0118 (HW), and the Deutsche Forschungsgemeinschaft (DFG) for financial support under Grant Number Sp314/13-1.

**Institutional Review Board Statement:** Not applicable.

**Informed Consent Statement:** Not applicable.

**Data Availability Statement:** Spectroscopic data for latrunculin A and other relevant information for all conducted experiments are provided. The organisms are listed in the collection event list of the Reference Collection of Sam Ratulangi University, Manado, Indonesia (SRU2015/01 SRU2016/02). Collection permits for all collected samples were provided by the Bunaken National Marine Park Authority for 2015 (SI.272/BTNB/PK/2015) and for 2016 (SI.399/BTNB/PK/2016).

**Acknowledgments:** We thank Carola Greve for providing the living *Elysia viridis* specimen, and Gregor Christa for providing *E. viridis* gDNA. Dario Karmeinski kindly provided transcriptomic cDNA sequences of Cladobranchia species. Furthermore, we would like to thank Dirk Erpenbeck for identifying the sponge sample as *Cacospongia mycofijiensis*. We also thank Hanns Häberlein and Sebastian Franken for their support with the fluorescence microscopy, and Bernhard Spengler for his support with MALDI-MS imaging. Furthermore, we thank the reviewers for their insightful comments and suggestions, which led to an improved version of this manuscript. We would like to express our special gratitude to our departed colleague Fontje Kaligis (Faculty of Fishery and Marine Sciences, Sam Ratulangi University, Manado), who supported us in all aspects of the INDOBIO-

collaboration and also provided *Chromodoris* sea slugs for this study. We are very grateful to Frans Gruber Ijong and the Politeknik Negeri Nusa Utara for all their support with the work on Kepulauan Sangihe and to Markus Lasut and Grevo Gerung (Faculty of Fishery and Marine Sciences, Sam Ratulangi University, Manado) for continued support and assistance with the ABS paperwork to follow the Nagoya Protocol. Finally, we are grateful to the Republic of Indonesia for making this research possible.

**Conflicts of Interest:** D.R. Bhandari was a part-time employee of TransMIT GmbH, Giessen. All other authors declare no conflicts of interest.

## References

1. Wägele, H.; Klussmann-Kolb, A. Opisthobranchia (Mollusca, Gastropoda)—More than Just Slimy Slugs. Shell Reduction and Its Implications on Defence and Foraging. *Front. Zool.* **2005**, *2*, 3. [CrossRef]
2. Faulkner, D.; Ghiselin, M. Chemical Defense and Evoluti—Onary Ecology of Dorid Nudibranchs and Some Other Opisthobranch Gastropods. *Mar. Ecol. Prog. Ser.* **1983**, *13*, 295–301. [CrossRef]
3. Avila, C.; Núñez-Pons, L.; Moles, J. From the Tropics to the Poles: Chemical Defense Strategies in Sea Slugs (Mollusca: Heterobranchia). In *Chemical Ecology*; CRC Press: Boca Raton, FL, USA, 2018; ISBN 978-0-429-45346-5.
4. Dietz, L.; Dömel, J.S.; Leese, F.; Lehmann, T.; Melzer, R.R. Feeding Ecology in Sea Spiders (Arthropoda: Pycnogonida): What Do We Know? *Front. Zool.* **2018**, *15*, 7. [CrossRef]
5. Mehrotra, R.; Monchanin, C.; Scott, C.M.; Phongsuwan, N.; Gutierrez, M.C.; Chavanich, S.; Hoeksema, B.W. Selective Consumption of Sacoglossan Sea Slugs (Mollusca: Gastropoda) by Scleractinian Corals (Cnidaria: Anthozoa). *PLoS ONE* **2019**, *14*, e0215063. [CrossRef]
6. Anker, A.; Ivanov, Y. First Record of the Predation upon Sea Slugs (Cephalaspidea and Nudibranchia) by the Peculiar Elbow Crab Lambrachaeus Ramifer Alcock, 1895 (Decapoda: Parthenopidae). *Mar. Biodivers.* **2020**, *50*, 24. [CrossRef]
7. Battini, N.; Bravo, G. Unexpected Meal: First Record of Predation upon a Potentially Neurotoxic Sea Slug by the European Green Crab Carcinus Maenas. *N. Z. J. Zool.* **2020**, *48*, 166–173. [CrossRef]
8. Battini, N.; Giachetti, C.; Castro, K.; Bortolus, A.; Schwindt, E. Predator–Prey Interactions as Key Drivers for the Invasion Success of a Potentially Neurotoxic Sea Slug. *Biol. Invasions* **2021**, *23*, 1–23. [CrossRef]
9. Avila, C. Natural Products of Opisthobranch Molluscs: A Biological Review. In *Oceanography and Marine Biology—An Annual Review, Vol 33*; Ansell, A.D., Gibson, R.N., Barnes, M., Eds.; U C L Press Ltd: London, UK, 1995; Volume 33, pp. 487–559, ISBN 978-1-85728-363-1.
10. Cimino, G.; Ghiselin, M.T. Chemical Defense and Evolutionary Trends in Biosynthetic Capacity among Dorid Nudibranchs (Mollusca: Gastropoda: Opisthobranchia). *Chemoecology* **1999**, *9*, 187–207. [CrossRef]
11. Cheney, K.L.; White, A.; Mudianta, I.W.; Winters, A.E.; Quezada, M.; Capon, R.J.; Mollo, E.; Garson, M.J. Choose Your Weaponry: Selective Storage of a Single Toxic Compound, Latrunculin A, by Closely Related Nudibranch Molluscs. *PLoS ONE* **2016**, *11*, e0145134. [CrossRef]
12. Dean, L.J.; Prinsep, M.R. The Chemistry and Chemical Ecology of Nudibranchs. *Nat. Prod. Rep.* **2017**, *34*, 1359–1390. [CrossRef]
13. Fisch, K.M.; Hertzer, C.; Böhringer, N.; Wuisan, Z.G.; Schillo, D.; Bara, R.; Kaligis, F.; Wägele, H.; König, G.M.; Schäberle, T.F. The Potential of Indonesian Heterobranchs Found around Bunaken Island for the Production of Bioactive Compounds. *Mar. Drugs* **2017**, *15*, 384. [CrossRef]
14. Avila, C.; Angulo-Preckler, C. Bioactive Compounds from Marine Heterobranchs. *Mar. Drugs* **2020**, *2020*, 657. [CrossRef]
15. Winters, A.E.; Chan, W.; White, A.M.; van den Berg, C.P.; Garson, M.J.; Cheney, K.L. Weapons or Deterrents? Nudibranch Molluscs Use Distinct Ecological Modes of Chemical Defence against Predators. *J. Anim. Ecol.* **2022**, *91*, 831–844. [CrossRef]
16. Johnson, R.F.; Gosliner, T.M. Traditional Taxonomic Groupings Mask Evolutionary History: A Molecular Phylogeny and New Classification of the Chromodorid Nudibranchs. *PLoS ONE* **2012**, *7*, e33479. [CrossRef]
17. Layton, K.K.S.; Gosliner, T.M.; Wilson, N.G. Flexible Colour Patterns Obscure Identification and Mimicry in Indo-Pacific Chromodoris Nudibranchs (Gastropoda: Chromodorididae). *Mol. Phylogenet. Evol.* **2018**, *124*, 27–36. [CrossRef]
18. Undap, N.; Papu, A.; Schillo, D.; Ijong, F.G.; Kaligis, F.; Lepar, M.; Hertzer, C.; Böhringer, N.; König, G.M.; Schäberle, T.F.; et al. First Survey of Heterobranch Sea Slugs (Mollusca, Gastropoda) from the Island Sangihe, North Sulawesi, Indonesia. *Diversity* **2019**, *11*, 170. [CrossRef]
19. Layton, K.; Carvajal, J.; Wilson, N. Mimicry and Mitonuclear Discordance in Nudibranchs: New Insights from Exon Capture Phylogenomics. *Ecol. Evol.* **2020**, *10*, 11966–11982. [CrossRef]
20. Padula, V.; Bahia, J.; Stöger, I.; Camacho-García, Y.; Malaquias, M.A.E.; Cervera, J.L.; Schrödl, M. A Test of Color-Based Taxonomy in Nudibranchs: Molecular Phylogeny and Species Delimitation of the Felimida Clenchi (Mollusca: Chromodorididae) Species Complex. *Mol. Phylogenet. Evol.* **2016**, *103*, 215–229. [CrossRef]
21. Nakano, R.; Hirose, E. Field Experiments on the Feeding of the Nudibranch Gymnodoris Spp. (Nudibranchia: Doridina: Gymnodorididae) in Japan. *Veliger* **2011**, *51*, 66–75.
22. Avila, C. Terpenoids in Marine Heterobranch Molluscs. *Mar. Drugs* **2020**, *18*, 162. [CrossRef]

23. Pawlik, J.R.; Kernan, M.R.; Molinski, T.F.; Harper, M.K.; Faulkner, D.J. Defensive Chemicals of the Spanisch Dancer Nudibranch Hexabranchus Sanguineus and Its Egg Ribbons: Macrolides Derived from a Sponge Diet. *J. Exp. Mar. Biol. Ecol.* **1988**, *119*, 99–109. [CrossRef]
24. Proksch, P. Defensive Roles for Secondary Metabolites from Marine Sponges and Sponge-Feeding Nudibranchs. *Toxicon* **1994**, *32*, 639–655. [CrossRef]
25. Taylor, M.W.; Radax, R.; Steger, D.; Wagner, M. Sponge-Associated Microorganisms: Evolution, Ecology, and Biotechnological Potential. *Microbiol. Mol. Biol. Rev.* **2007**, *71*, 295–347. [CrossRef]
26. Taylor, M.W.; Hill, R.T.; Piel, J.; Thacker, R.W.; Hentschel, U. Soaking It up: The Complex Lives of Marine Sponges and Their Microbial Associates. *ISME J.* **2007**, *1*, 187–190. [CrossRef]
27. Putz, A.; Proksch, P. Chemical Defence in Marine Ecosystems. In *Annual Plant Reviews Volume 39: Functions and Biotechnology of Plant Secondary Metabolites*; John Wiley & Sons, Ltd.: Hoboken, NJ, USA, 2010; pp. 162–213, ISBN 978-1-4443-1887-6.
28. Ng, T.P.T.; Saltin, S.H.; Davies, M.S.; Johannesson, K.; Stafford, R.; Williams, G.A. Snails and Their Trails: The Multiple Functions of Trail-Following in Gastropods. *Biol. Rev.* **2013**, *88*, 683–700. [CrossRef]
29. Puglisi, M.P.; Sneed, J.M.; Sharp, K.H.; Ritson-Williams, R.; Paul, V.J. Marine Chemical Ecology in Benthic Environments. *Nat. Prod. Rep.* **2014**, *31*, 1510–1553. [CrossRef]
30. Mollo, E.; Fontana, A.; Roussis, V.; Polese, G.; Amodeo, P.; Ghiselin, M.T. Sensing Marine Biomolecules: Smell, Taste, and the Evolutionary Transition from Aquatic to Terrestrial Life. *Chem. Biol.* **2014**, *2*, 92. [CrossRef]
31. Rohde, S.; Nietzer, S.; Schupp, P.J. Prevalence and Mechanisms of Dynamic Chemical Defenses in Tropical Sponges. *PLoS ONE* **2015**, *10*, e0132236. [CrossRef]
32. Venuleo, M.; Raven, J.A.; Giordano, M. Intraspecific Chemical Communication in Microalgae. *New Phytol.* **2017**, *215*, 516–530. [CrossRef]
33. Müller, C.; Caspers, B.A.; Gadau, J.; Kaiser, S. The Power of Infochemicals in Mediating Individualized Niches. *Trends Ecol. Evol.* **2020**, *35*, 981–989. [CrossRef]
34. Okuda, R.K. Chemical Ecology of Some Opisthobranch Mollusks. Ph.D. Thesis, University of Hawai'i at Manoa, Honolulu, HI, USA, 1983.
35. Okuda, R.K.; Scheuer, P.J. Latrunculin-A, Ichthyotoxic Constituent of the NudibranchChromodoris Elisabethina. *Experientia* **1985**, *41*, 1355–1356. [CrossRef]
36. Pika, J.; John Faulkner, D. Unusual Chlorinated Homo-Diterpenes from the South African Nudibranch Chromodoris Hamiltoni. *Tetrahedron* **1995**, *51*, 8189–8198. [CrossRef]
37. Kakou, Y.; Crews, P.; Bakus, G.J. Dendrolasin and Latrunculin A from the Fijian Sponge Spongia Mycofijiensis and an Associated Nudibranch Chromodoris Lochi. *J. Nat. Prod.* **1987**, *50*, 482–484. [CrossRef]
38. Houssen, W.E.; Jaspars, M.; Wease, K.N.; Scott, R.H. Acute Actions of Marine Toxin Latrunculin A on the Electrophysiological Properties of Cultured Dorsal Root Ganglion Neurones. *Comp. Biochem. Physiol. Toxicol. Pharmacol. CBP* **2006**, *142*, 19–29. [CrossRef]
39. Hamilton, B.R.; Chan, W.; Cheney, K.L.; Sullivan, R.K.P.; Floetenmeyer, M.; Garson, M.J.; Wepf, R. Cryo-Ultramicrotomy and Mass Spectrometry Imaging Analysis of Nudibranch Microstructures. *J. Am. Soc. Mass Spectrom.* **2022**, *33*, 592–597. [CrossRef]
40. McPhail, K.; Davies-Coleman, M.T. New Spongiane Diterpenes from the East African Nudibranch Chromodoris Hamiltoni. *Tetrahedron* **1997**, *53*, 4655–4660. [CrossRef]
41. Mebs, D. Chemical Defense of a Dorid Nudibranch, Glossodoris Quadricolor, from the Red Sea. *J. Chem. Ecol.* **1985**, *11*, 713–716. [CrossRef]
42. Ilan, M. Reproductive Biology, Taxonomy, and Aspects of Chemical Ecology of Latrunculiidae (Porifera). *Biol. Bull.* **1995**, *188*, 306–312. [CrossRef]
43. Guo, Y. Chemical Studies of the Novel Bioactive Secondary Metabolites from the Benthic Invertebrates: Isolation and Structure Characterization. Ph.D. Thesis, University of Naples, Naples, Italy, 1997.
44. Amagata, T.; Johnson, T.A.; Cichewicz, R.H.; Tenney, K.; Mooberry, S.L.; Media, J.; Edelstein, M.; Valeriote, F.A.; Crews, P. Interrogating the Bioactive Pharmacophore of the Latrunculin Chemotype by Investigating the Metabolites of Two Taxonomically Unrelated Sponges. *J. Med. Chem.* **2008**, *51*, 7234–7242. [CrossRef]
45. Sonnenschein, R.N.; Johnson, T.A.; Tenney, K.; Valeriote, F.A.; Crews, P. A Reassignment of (–)-Mycothiazole and the Isolation of a Related Diol. *J. Nat. Prod.* **2006**, *69*, 145–147. [CrossRef]
46. Kashman, Y.; Groweiss, A.; Shmueli, U. Latrunculin, a New 2-Thiazolidinone Macrolide from the Marine Sponge Latrunculia Magnifica. *Tetrahedron Lett.* **1980**, *21*, 3629–3632. [CrossRef]
47. Spector, I.; Shochet, N.R.; Kashman, Y.; Groweiss, A. Latrunculins: Novel Marine Toxins That Disrupt Microfilament Organization in Cultured Cells. *Science* **1983**, *219*, 493–495. [CrossRef]
48. Smith, A.B.; Leahy, J.W.; Noda, I.; Remiszewski, S.W.; Liverton, N.J.; Zibuck, R. Total Synthesis of the Latrunculins. *J. Am. Chem. Soc.* **1992**, *114*, 2995–3007. [CrossRef]
49. Oliveira, C.A.; Kashman, Y.; Mantovani, B. Effects of Latrunculin A on Immunological Phagocytosis and Macrophage Spreading-Associated Changes in the F-Actin/G-Actin Content of the Cells. *Chem. Biol. Interact.* **1996**, *100*, 141–153. [CrossRef]
50. Tanaka, J.; Higa, T.; Bernardinelli, G.; Jefford, C.W. New Cytotoxic Macrolides from the Sponge Fasciospongia Rimosa. *Chem. Lett.* **1996**, *25*, 255–256. [CrossRef]

51. Ayscough, K.R.; Stryker, J.; Pokala, N.; Sanders, M.; Crews, P.; Drubin, D.G. High Rates of Actin Filament Turnover in Budding Yeast and Roles for Actin in Establishment and Maintenance of Cell Polarity Revealed Using the Actin Inhibitor Latrunculin-A. *J. Cell Biol.* **1997**, *137*, 399–416. [CrossRef]
52. Belmont, L.D.; Patterson, G.M.; Drubin, D.G. New Actin Mutants Allow Further Characterization of the Nucleotide Binding Cleft and Drug Binding Sites. *J. Cell Sci.* **1999**, *112 Pt 9*, 1325–1336. [CrossRef]
53. Cai, S.; Liu, X.; Glasser, A.; Volberg, T.; Filla, M.; Geiger, B.; Polansky, J.R.; Kaufman, P.L. Effect of Latrunculin-A on Morphology and Actin-Associated Adhesions of Cultured Human Trabecular Meshwork Cells. *Mol. Vis.* **2000**, *6*, 132–143.
54. Gillor, O.; Carmeli, S.; Rahamim, Y.; Fishelson, Z.; Ilan, M. Immunolocalization of the Toxin Latrunculin B within the Red Sea Sponge Negombata Magnifica (Demospongiae, Latrunculiidae). *Mar. Biotechnol.* **2000**, *2*, 213–223. [CrossRef]
55. Morton, W.M.; Ayscough, K.R.; McLaughlin, P.J. Latrunculin Alters the Actin-Monomer Subunit Interface to Prevent Polymerization. *Nat. Cell Biol.* **2000**, *2*, 376–378. [CrossRef]
56. Yarmola, E.G.; Somasundaram, T.; Boring, T.A.; Spector, I.; Bubb, M.R. Actin-Latrunculin A Structure and Function. Differential Modulation of Actin-Binding Protein Function by Latrunculin, A.J. *Biol. Chem.* **2000**, *275*, 28120–28127. [CrossRef]
57. Baluška, F.; Jasik, J.; Edelmann, H.G.; Salajová, T.; Volkmann, D. Latrunculin B-Induced Plant Dwarfism: Plant Cell Elongation Is F-Actin-Dependent. *Dev. Biol.* **2001**, *231*, 113–124. [CrossRef]
58. Wakatsuki, T.; Schwab, B.; Thompson, N.C.; Elson, E.L. Effects of Cytochalasin D and Latrunculin B on Mechanical Properties of Cells. *J. Cell Sci.* **2001**, *114*, 1025–1036. [CrossRef]
59. Pring, M.; Cassimeris, L.; Zigmond, S.H. An Unexplained Sequestration of Latrunculin A Is Required in Neutrophils for Inhibition of Actin Polymerization. *Cell Motil. Cytoskeleton* **2002**, *52*, 122–130. [CrossRef]
60. Fujita, M.; Ichinose, S.; Kiyono, T.; Tsurumi, T.; Omori, A. Establishment of Latrunculin-A Resistance in HeLa Cells by Expression of R183A D184A Mutant Beta-Actin. *Oncogene* **2003**, *22*, 627–631. [CrossRef]
61. Vilozny, B.; Amagata, T.; Mooberry, S.L.; Crews, P. A New Dimension to the Biosynthetic Products Isolated from the Sponge Negombata Magnifica. *J. Nat. Prod.* **2004**, *67*, 1055–1057. [CrossRef]
62. Ethier, C.R.; Read, A.T.; Chan, D.W.-H. Effects of Latrunculin-B on Outflow Facility and Trabecular Meshwork Structure in Human Eyes. *Investig. Ophthalmol. Vis. Sci.* **2006**, *47*, 1991–1998. [CrossRef]
63. El Sayed, K.A.; Youssef, D.T.A.; Marchetti, D. Bioactive Natural and Semisynthetic Latrunculins. *J. Nat. Prod.* **2006**, *69*, 219–223. [CrossRef]
64. Khalifa, S.; Ahmed, S.; Mesbah, M.; Youssef, D.; Hamann, M. Quantitative Determination of Latrunculins A and B in the Red Sea Sponge Negombata Magnifica by High Performance Liquid Chromatography. *J. Chromatogr. B* **2006**, *832*, 47–51. [CrossRef]
65. Sierra-Paredes, G.; Oreiro-García, T.; Núñez-Rodriguez, A.; Vázquez-López, A.; Sierra-Marcuño, G. Seizures Induced by in Vivo Latrunculin A and Jasplakinolide Microperfusion in the Rat Hippocampus. *J. Mol. Neurosci.* **2006**, *28*, 151–160. [CrossRef]
66. Foissner, I.; Wasteneys, G.O. Wide-Ranging Effects of Eight Cytochalasins and Latrunculin A and B on Intracellular Motility and Actin Filament Reorganization in Characean Internodal Cells. *Plant Cell Physiol.* **2007**, *48*, 585–597. [CrossRef]
67. Fürstner, A.; Kirk, D.; Fenster, M.D.B.; Aïssa, C.; De Souza, D.; Nevado, C.; Tuttle, T.; Thiel, W.; Müller, O. Latrunculin Analogues with Improved Biological Profiles by "Diverted Total Synthesis": Preparation, Evaluation, and Computational Analysis. *Chem.—Eur. J.* **2007**, *13*, 135–149. [CrossRef]
68. Meadows, J.C.; Millar, J.; Solomon, M. Latrunculin A Delays Anaphase Onset in Fission Yeast by Disrupting an Ase1-Independent Pathway Controlling Mitotic Spindle Stability. *Mol. Biol. Cell* **2008**, *19*, 3713–3723. [CrossRef]
69. Konishi, H.; Kikuchi, S.; Ochiai, T.; Ikoma, H.; Kubota, T.; Ichikawa, D.; Fujiwara, H.; Okamoto, K.; Sakakura, C.; Sonoyama, T.; et al. Latrunculin A Has a Strong Anticancer Effect in a Peritoneal Dissemination Model of Human Gastric Cancer in Mice. *Anticancer Res.* **2009**, *29*, 2091–2097.
70. Kudrimoti, S.; Ahmed, S.A.; Daga, P.R.; Wahba, A.E.; Khalifa, S.I.; Doerksen, R.J.; Hamann, M.T. Semisynthetic Latrunculin B Analogs: Studies of Actin Docking Support a Proposed Mechanism for Latrunculin Bioactivity. *Bioorg. Med. Chem.* **2009**, *17*, 7517–7522. [CrossRef]
71. Ketelaar, T.; Meijer, H.J.G.; Spiekerman, M.; Weide, R.; Govers, F. Effects of Latrunculin B on the Actin Cytoskeleton and Hyphal Growth in Phytophthora Infestans. *Fungal Genet. Biol.* **2012**, *49*, 1014–1022. [CrossRef]
72. Saito, S. Toxins Affecting Actin Filaments and Microtubules. In *Marine Toxins as Research Tools*; Fusetani, N., Kem, W., Eds.; Progress in Molecular and Subcellular Biology; Springer: Berlin/Heidelberg, Germany, 2009; Volume 46, pp. 187–219, ISBN 978-3-540-87892-6.
73. Moscatelli, A.; Idilli, A.I.; Rodighiero, S.; Caccianiga, M. Inhibition of Actin Polymerisation by Low Concentration Latrunculin B Affects Endocytosis and Alters Exocytosis in Shank and Tip of Tobacco Pollen Tubes. *Plant Biol.* **2012**, *14*, 770–782. [CrossRef]
74. Terashita, Y.; Yamagata, K.; Tokoro, M.; Itoi, F.; Wakayama, S.; Li, C.; Sato, E.; Tanemura, K.; Wakayama, T. Latrunculin A Treatment Prevents Abnormal Chromosome Segregation for Successful Development of Cloned Embryos. *PLoS ONE* **2013**, *8*, e78380. [CrossRef]
75. Kopecká, M.; Yamaguchi, M.; Kawamoto, S. Effects of the F-Actin Inhibitor Latrunculin A on the Budding Yeast Saccharomyces Cerevisiae. *Microbiol. Read. Engl.* **2015**, *161*, 1348–1355. [CrossRef]
76. Ebrahim, H.Y.; El Sayed, K.A. Discovery of Novel Antiangiogenic Marine Natural Product Scaffolds. *Mar. Drugs* **2016**, *14*, 57. [CrossRef]

77. Varghese, S.; Rahmani, R.; Drew, D.; Williams, M.; Huang, J.; Wilkinson, M.; Tan, Y.-H.; Tonkin, C.; Beeson, J.; Baum, J.; et al. Truncated Latrunculins as Actin Inhibitors Targeting Plasmodium Falciparum Motility and Host-Cell Invasion. *J. Med. Chem.* **2016**, *59*, 10994–11005. [CrossRef]
78. da Silva, S.C.G.P. Multi-Approach Analysis of the Metagenome of a Marine Sponge Containing Latrunculin A. Master's Thesis, Ciências Farmacêuticas, Universidade de Lisboa, Faculdade de Farmácia, Lisbon, Portugal, 2017.
79. Fujiwara, I.; Zweifel, M.E.; Courtemanche, N.; Pollard, T.D. Latrunculin A Accelerates Actin Filament Depolymerization in Addition to Sequestering Actin Monomers. *Curr. Biol. CB* **2018**, *28*, 3183–3192. [CrossRef]
80. Würtemberger, J.; Tchessalova, D.; Regina, C.; Bauer, C.; Schneider, M.; Wagers, A.J.; Hettmer, S. Growth Inhibition Associated with Disruption of the Actin Cytoskeleton by Latrunculin A in Rhabdomyosarcoma Cells. *PLoS ONE* **2020**, *15*, e0238572. [CrossRef]
81. Al-Tarabeen, M.; El-Neketi, M.; Albohy, A.; Müller, W.E.G.; Rasheed, M.; Ebrahim, W.; Proksch, P.; Ebada, S.S. Isolation and Molecular Docking of Cytotoxic Secondary Metabolites from Two Red Sea Sponges of the Genus Diacarnus. *ChemistrySelect* **2021**, *6*, 217–220. [CrossRef]
82. Lenz, K.D.; Klosterman, K.E.; Mukundan, H.; Kubicek-Sutherland, J.Z. Macrolides: From Toxins to Therapeutics. *Toxins* **2021**, *13*, 347. [CrossRef]
83. Varghese, S.; Rahmani, R.; Drew, D.R.; Beeson, J.G.; Baum, J.; Smith, B.J.; Baell, J.B. Structure-Activity Studies of Truncated Latrunculin Analogues with Antimalarial Activity. *ChemMedChem* **2021**, *16*, 679–693. [CrossRef]
84. Risinger, A.L.; Du, L. Targeting and Extending the Eukaryotic Druggable Genome with Natural Products: Cytoskeletal Targets of Natural Products. *Nat. Prod. Rep.* **2019**, 634–652. [CrossRef]
85. Rubenstein, P.A. The Functional Importance of Multiple Actin Isoforms. *BioEssays* **1990**, *12*, 309–315. [CrossRef]
86. Doolittle, R.F.; Gerhart, J.; Hunt, R.T.; Kirschner, M.W.; Wolpert, L. The Origins and Evolution of Eukaryotic Proteins. *Philos. Trans. R. Soc. Lond. B. Biol. Sci.* **1995**, *349*, 235–240. [CrossRef]
87. Lodish, H.; Berk, A.; Zipursky, S.L.; Matsudaira, P.; Baltimore, D.; Darnell, J. *Mol. Cell Biol.*, 4th ed.; W. H. Freeman: New York, NY, USA, 2000; ISBN 978-0-7167-3136-8.
88. Chhabra, E.S.; Higgs, H.N. The Many Faces of Actin: Matching Assembly Factors with Cellular Structures. *Nat. Cell Biol.* **2007**, *9*, 1110–1121. [CrossRef]
89. Perrin, B.J.; Ervasti, J.M. The Actin Gene Family: Function Follows Isoform. *Cytoskelet. Hoboken Nj* **2010**, *67*, 630–634. [CrossRef]
90. Dominguez, R.; Holmes, K.C. Actin Structure and Function. *Annu. Rev. Biophys.* **2011**, *40*, 169–186. [CrossRef]
91. Gunning, P.W.; Ghoshdastider, U.; Whitaker, S.; Popp, D.; Robinson, R.C. The Evolution of Compositionally and Functionally Distinct Actin Filaments. *J. Cell Sci.* **2015**, *128*, 2009–2019. [CrossRef]
92. Skau, C.T.; Waterman, C.M. Specification of Architecture and Function of Actin Structures by Actin Nucleation Factors. *Annu. Rev. Biophys.* **2015**, *44*, 285–310. [CrossRef]
93. Pollard, T.D. Actin and Actin-Binding Proteins. *Cold Spring Harb. Perspect. Biol.* **2016**, *8*, a018226. [CrossRef]
94. Parisis, N.; Krasinska, L.; Harker, B.; Urbach, S.; Rossignol, M.; Camasses, A.; Dewar, J.; Morin, N.; Fisher, D. Initiation of DNA Replication Requires Actin Dynamics and Formin Activity. *EMBO J.* **2017**, *36*, 3212–3231. [CrossRef]
95. Pollard, T.D. What We Know and Do Not Know About Actin. *Handb. Exp. Pharmacol.* **2017**, *235*, 331–347. [CrossRef]
96. Stoddard, P.R.; Williams, T.A.; Garner, E.; Baum, B. Evolution of Polymer Formation within the Actin Superfamily. *Mol. Biol. Cell* **2017**, *28*, 2461–2469. [CrossRef]
97. Vedula, P.; Kashina, A. The Makings of the 'actin Code': Regulation of Actin's Biological Function at the Amino Acid and Nucleotide Level. *J. Cell Sci.* **2018**, *131*, jcs215509. [CrossRef]
98. Wada, S.; Matsunaga, S.; Saito, S.; Fusetani, N.; Watabe, S. Actin-Binding Specificity of Marine Macrolide Toxins, Mycalolide B and Kabiramide D. *J. Biochem.* **1998**, *123*, 946–952. [CrossRef]
99. Belmont, L.D.; Drubin, D.G. The Yeast V159N Actin Mutant Reveals Roles for Actin Dynamics In Vivo. *J. Cell Biol.* **1998**, *142*, 1289–1299. [CrossRef]
100. Procaccio, V.; Salazar, G.; Ono, S.; Styers, M.L.; Gearing, M.; Davila, A.; Jimenez, R.; Juncos, J.; Gutekunst, C.-A.; Meroni, G.; et al. A Mutation of β-Actin That Alters Depolymerization Dynamics Is Associated with Autosomal Dominant Developmental Malformations, Deafness, and Dystonia. *Am. J. Hum. Genet.* **2006**, *78*, 947–960. [CrossRef]
101. Schwarzerová, K.; Vondráková, Z.; Fischer, L.; Bořiková, P.; Bellinvia, E.; Eliášová, K.; Havelková, L.; Fišerová, J.; Vágner, M.; Opatrný, Z. The Role of Actin Isoforms in Somatic Embryogenesis in Norway Spruce. *BMC Plant Biol.* **2010**, *10*, 89. [CrossRef]
102. Rivière, J.-B.; van Bon, B.W.M.; Hoischen, A.; Kholmanskikh, S.S.; O'Roak, B.J.; Gilissen, C.; Gijsen, S.; Sullivan, C.T.; Christian, S.L.; Abdul-Rahman, O.A.; et al. De Novo Mutations in the Actin Genes ACTB and ACTG1 Cause Baraitser-Winter Syndrome. *Nat. Genet.* **2012**, *44*, 440-S2. [CrossRef]
103. Johnston, J.J.; Wen, K.-K.; Keppler-Noreuil, K.; McKane, M.; Maiers, J.L.; Greiner, A.; Sapp, J.C.; NIH Intramural Sequencing Center; Demali, K.A.; Rubenstein, P.A.; et al. Functional Analysis of a de Novo ACTB Mutation in a Patient with Atypical Baraitser-Winter Syndrome. *Hum. Mutat.* **2013**, *34*, 1242–1249. [CrossRef]
104. Roopa, L.; Pravin, K.R.; Sudheer Mohammed, M.M. Molecular Dynamics Simulation Reveal the Mechanism of Resistance of Mutant Actins to Latrunculin A—Insight into Specific Modifications to Design Novel Drugs to Overcome Resistance. *Curr. Comput. Aided Drug Des.* **2016**, *12*, 107–118.

105. Filipuzzi, I.; Thomas, J.R.; Pries, V.; Estoppey, D.; Salcius, M.; Studer, C.; Schirle, M.; Hoepfner, D. Direct Interaction of Chivosazole F with Actin Elicits Cell Responses Similar to Latrunculin A but Distinct from Chondramide. *ACS Chem. Biol.* **2017**, *12*, 2264–2269. [CrossRef]
106. Singh, H.P.; Batish, D.R.; Kohli, R.K. Autotoxicity: Concept, Organisms, and Ecological Significance. *Crit. Rev. Plant Sci.* **1999**, *18*, 757–772. [CrossRef]
107. Arbuckle, K.; Rodríguez de la Vega, R.C.; Casewell, N.R. Coevolution Takes the Sting out of It: Evolutionary Biology and Mechanisms of Toxin Resistance in Animals. *Toxicon* **2017**, *140*, 118–131. [CrossRef]
108. Almabruk, K.H.; Dinh, L.K.; Philmus, B. Self-Resistance of Natural Product Producers: Past, Present, and Future Focusing on Self-Resistant Protein Variants. *ACS Chem. Biol.* **2018**, *13*, 1426–1437. [CrossRef]
109. Ogawara, H. Comparison of Strategies to Overcome Drug Resistance: Learning from Various Kingdoms. *Mol. J. Synth. Chem. Nat. Prod. Chem.* **2018**, *23*, 1476. [CrossRef]
110. Yan, Y.; Liu, N.; Tang, Y. Recent Developments in Self-Resistance Gene Directed Natural Product Discovery. *Nat. Prod. Rep.* **2020**, *37*, 879–892. [CrossRef]
111. Crozier, W.J.; Crozier, W.J. The Nature of the Conical Bodies on the Mantle of Certain Nudibranchs. *Nautilus* **1917**, *30*, 103–106.
112. Groweiss, A.; Shmueli, U.; Kashman, Y. Marine Toxins of Latrunculia Magnifica. *J. Org. Chem.* **1983**, *48*, 3512–3516. [CrossRef]
113. Garson, M.J.; Thompson, J.E.; Larsen, R.M.; Battershill, C.N.; Murphy, P.T.; Bergquist, P.R. Terpenes in Sponge Cell Membranes: Cell Separation and Membrane Fractionation Studies with the Tropical Marine SpongeAmphimedon Sp. *Lipids* **1992**, *27*, 378–388. [CrossRef]
114. Uriz, M.J.; Becerro, M.A.; Tur, J.M.; Turon, X. Location of Toxicity within the Mediterranean Sponge Crambe Crambe (Demospongiae: Poecilosclerida). *Mar. Biol.* **1996**, *124*, 583–590. [CrossRef]
115. Uriz, M.J.; Turon, X.; Galera, J.; Tur, J.M. New Light on the Cell Location of Avarol within the Sponge Dysidea Avara (Dendroceratida). *Cell Tissue Res.* **1996**, *285*, 519–527. [CrossRef]
116. Garson, M.J.; Flowers, A.E.; Webb, R.I.; Charan, R.D.; McCaffrey, E.J. A Sponge/Dinoflagellate Association in the Haplosclerid Sponge Haliclona Sp.: Cellular Origin of Cytotoxic Alkaloids by Percoll Density Gradient Fractionation. *Cell Tissue Res.* **1998**, *293*, 365–373. [CrossRef]
117. Turon, X.; Becerro, M.A.; Uriz, M.J. Distribution of Brominated Compounds within the Sponge Aplysina Aerophoba: Coupling of X-Ray Microanalysis with Cryofixation Techniques. *Cell Tissue Res.* **2000**, *301*, 311–322. [CrossRef]
118. Gerçe, B.; Schwartz, T.; Voigt, M.; Rühle, S.; Kirchen, S.; Putz, A.; Proksch, P.; Obst, U.; Syldatk, C.; Hausmann, R. Morphological, Bacterial, and Secondary Metabolite Changes of Aplysina Aerophoba upon Long-Term Maintenance Under Artificial Conditions. *Microb. Ecol.* **2009**, *58*, 865–878. [CrossRef]
119. Tianero, M.D.; Balaich, J.N.; Donia, M.S. Localized Production of Defence Chemicals by Intracellular Symbionts of Haliclona Sponges. *Nat. Microbiol.* **2019**, *4*, 1149–1159. [CrossRef]
120. Avila, C.; Cimino, G.; Fontana, A.; Gavagnin, M.; Ortea, J.; Trivellone, E. Defensive Strategy of Two Hypselodoris Nudibranchs from Italian and Spanish Coasts. *J. Chem. Ecol.* **1991**, *17*, 625–636. [CrossRef]
121. García-Gómez, J.C.; Cimino, G.; Medina, A. Studies on the Defensive Behaviour of Hypselodoris Species (Gastropoda: Nudibranchia): Ultrastructure and Chemical Analysis of Mantle Dermal Formations (MDFs). *Mar. Biol.* **1990**, *106*, 245–250. [CrossRef]
122. Fontana, A.; Giménez, F.; Marin, A.; Mollo, E.; Cimino, G. Transfer of Secondary Metabolites from the Sponges Dysidea Fragilis and Pleraplysilla Spinifera to the Mantle Dermal Formations (MDFs) of the Mudibranch Hypserlodoris Webbi. *Experientia* **1994**, *50*, 510–516. [CrossRef]
123. Avila, C.; Paul, V.J. Chemical Ecology of the Nudibranch Glossodoris Pallida: Is the Location of Diet-Derived Metabolites Important for Defense? *Mar. Ecol. Prog. Ser.* **1997**, *150*, 171–180. [CrossRef]
124. Wägele, H.; Willan, R.C. Phylogeny of the Nudibranchia. *Zool. J. Linn. Soc.* **2000**, *130*, 83–181. [CrossRef]
125. Winters, A.E.; White, A.M.; Dewi, A.S.; Mudianta, I.W.; Wilson, N.G.; Forster, L.C.; Garson, M.J.; Cheney, K.L. Distribution of Defensive Metabolites in Nudibranch Molluscs. *J. Chem. Ecol.* **2018**, *44*, 384–396. [CrossRef]
126. Carbone, M.; Gavagnin, M.; Haber, M.; Guo, Y.-W.; Fontana, A.; Manzo, E.; Genta-Jouve, G.; Tsoukatou, M.; Rudman, W.B.; Cimino, G.; et al. Packaging and Delivery of Chemical Weapons: A Defensive Trojan Horse Stratagem in Chromodorid Nudibranchs. *PLoS ONE* **2013**, *8*, e62075. [CrossRef]
127. Wägele, H. Potential Key Characters in Opisthobranchia (Gastropoda, Mollusca) Enhancing Adaptive Radiation. *Org. Divers. Evol.* **2004**, *4*, 175–188. [CrossRef]
128. Winters, A.E.; Green, N.F.; Wilson, N.G.; How, M.J.; Garson, M.J.; Marshall, N.J.; Cheney, K.L. Stabilizing Selection on Individual Pattern Elements of Aposematic Signals. *Proc. R Soc. B* **2017**, *284*, 20170926. [CrossRef]
129. Wägele, H.; Ballesteros, M.; Avila, C. Defensive Glandular Structures In Opisthobranch Molluscs—From Histology To Ecology. *Oceanogr. Mar. Biol. Annu. Rev.* **2006**, *44*, 197–276. [CrossRef]
130. Eisenbarth, J.-H.; Undap, N.; Papu, A.; Schillo, D.; Dialao, J.; Reumschüssel, S.; Kaligis, F.; Bara, R.; Schäberle, T.F.; König, G.M.; et al. Marine Heterobranchia (Gastropoda, Mollusca) in Bunaken National Park, North Sulawesi, Indonesia—A Follow-Up Diversity Study. *Diversity* **2018**, *10*, 127. [CrossRef]
131. Kaligis, F.; Eisenbarth, J.-H.; Schillo, D.; Dialao, J.; Schäberle, T.F.; Böhringer, N.; Bara, R.; Reumschüssel, S.; König, G.M.; Wägele, H. Second Survey of Heterobranch Sea Slugs (Mollusca, Gastropoda, Heterobranchia) from Bunaken National Park, North Sulawesi, Indonesia—How Much Do We Know after 12 Years? *Mar. Biodivers. Rec.* **2018**, *11*, 2. [CrossRef]

132. Ackers, R.G.; Moss, D.; Picton, B.E.; Bt, B.; Stone, S.M.K.; Morrow, C.C. Sponges of the British Isles ("Sponge V") —A Colour Guide and Working Document, 1992 Edition. *Mar. Conserv. Soc.* **2007**, 165.
133. Erpenbeck, D.; Galitz, A.; Ekins, M.; Cook, S.D.C.; van Soest, R.W.M.; Hooper, J.N.A.; Wörheide, G. Soft Sponges with Tricky Tree: On the Phylogeny of Dictyoceratid Sponges. *J. Zool. Syst. Evol. Res.* **2020**, *58*, 27–40. [CrossRef]
134. Bouschen, W.; Schulz, O.; Eikel, D.; Spengler, B. Matrix Vapor Deposition/Recrystallization and Dedicated Spray Preparation for High-Resolution Scanning Microprobe Matrix-Assisted Laser Desorption/Ionization Imaging Mass Spectrometry (SMALDI-MS) of Tissue and Single Cells. *Rapid Commun. Mass Spectrom.* **2010**, *24*, 355–364. [CrossRef]
135. Koestler, M.; Kirsch, D.; Hester, A.; Leisner, A.; Guenther, S.; Spengler, B. A High-Resolution Scanning Microprobe Matrix-Assisted Laser Desorption/Ionization Ion Source for Imaging Analysis on an Ion Trap/Fourier Transform Ion Cyclotron Resonance Mass Spectrometer. *Rapid Commun. Mass Spectrom. RCM* **2008**, *22*, 3275–3285. [CrossRef]
136. Guenther, S.; Koestler, M.; Schulz, O.; Spengler, B. Laser Spot Size and Laser Power Dependence of Ion Formation in High Resolution MALDI Imaging. *Int. J. Mass Spectrom.* **2010**, *294*, 7–15. [CrossRef]
137. Römpp, A.; Guenther, S.; Schober, Y.; Schulz, O.; Takats, Z.; Kummer, W.; Spengler, B. Histology by Mass Spectrometry: Label-Free Tissue Characterization Obtained from High-Accuracy Bioanalytical Imaging. *Angew. Chem. Int. Ed.* **2010**, *49*, 3834–3838. [CrossRef]
138. Römpp, A.; Spengler, B. Mass Spectrometry Imaging with High Resolution in Mass and Space. *Histochem. Cell Biol.* **2013**, *139*, 759–783. [CrossRef]
139. Paschke, C.; Leisner, A.; Hester, A.; Maass, K.; Guenther, S.; Bouschen, W.; Spengler, B. Mirion—A Software Package for Automatic Processing of Mass Spectrometric Images. *J. Am. Soc. Mass Spectrom.* **2013**, *24*, 1296–1306. [CrossRef]
140. Database Resources of the National Center for Biotechnology Information. *Nucleic Acids Res.* **2018**, *46*, D8–D13. [CrossRef]
141. Karmeinski, D.; Meusemann, K.; Goodheart, J.A.; Schroedl, M.; Martynov, A.; Korshunova, T.; Wägele, H.; Donath, A. Transcriptomics Provides a Robust Framework for the Relationships of the Major Clades of Cladobranch Sea Slugs (Mollusca, Gastropoda, Heterobranchia), but Fails to Resolve the Position of the Enigmatic Genus Embletonia. *BMC Ecology and Evolution* **2021**, *21*, 226. [CrossRef]
142. DesGroseillers, L.; Auclair, D.; Wickham, L.; Maalouf, M. A Novel Actin CDNA Is Expressed in the Neurons of Aplysia Californica. *Biochim. Biophys. Acta* **1994**, *1217*, 322–324. [CrossRef]
143. Kumar, S.; Stecher, G.; Li, M.; Knyaz, C.; Tamura, K. MEGA X: Molecular Evolutionary Genetics Analysis across Computing Platforms. *Mol. Biol. Evol.* **2018**, *35*, 1547–1549. [CrossRef]
144. Huson, D.H.; Bryant, D. Application of Phylogenetic Networks in Evolutionary Studies. *Mol. Biol. Evol.* **2006**, *23*, 254–267. [CrossRef]
145. Larkin, M.A.; Blackshields, G.; Brown, N.P.; Chenna, R.; McGettigan, P.A.; McWilliam, H.; Valentin, F.; Wallace, I.M.; Wilm, A.; Lopez, R.; et al. Clustal W and Clustal X Version 2.0. *Bioinformatics* **2007**, *23*, 2947–2948. [CrossRef]
146. Kelley, L.A.; Mezulis, S.; Yates, C.M.; Wass, M.N.; Sternberg, M.J.E. The Phyre2 Web Portal for Protein Modeling, Prediction and Analysis. *Nat. Protoc.* **2015**, *10*, 845–858. [CrossRef]
147. White, J.D.; Kawasaki, M. Total Synthesis of (+)-Latrunculin A, an Ichthyotoxic Metabolite of the Sponge Latrunculia Magnifica and Its C-15 Epimer. *J. Org. Chem.* **1992**, *57*, 5292–5300. [CrossRef]
148. Fürstner, A.; De Souza, D.; Turet, L.; Fenster, M.D.B.; Parra-Rapado, L.; Wirtz, C.; Mynott, R.; Lehmann, C.W. Total Syntheses of the Actin-Binding Macrolides Latrunculin A, B, C, M, S and 16-Epi-Latrunculin B. *Chem. Weinh. Bergstr. Ger.* **2007**, *13*, 115–134. [CrossRef]
149. Rudman, W.B.; Bergquist, P.R. A Review of Feeding Specificity in the Sponge-Feeding Chromodorididae (Nudibranchia: Mollusca). *Molluscan Res.* **2007**, *27*, 60–88.
150. Putz, A.; König, G.M.; Wägele, H. Defensive Strategies of Cladobranchia (Gastropoda, Opisthobranchia). *Nat. Prod. Rep.* **2010**, *27*, 1386–1402. [CrossRef]
151. Wertman, K.F.; Drubin, D.G.; Botstein, D. Systematic Mutational Analysis of the Yeast ACT1 Gene. *Genetics* **1992**, *132*, 337–350. [CrossRef]
152. Rogers, S.D.; Paul, V.J. Chemical Defenses of Three Glossodoris Nudibranchs and Their Dietary Hyrtios Sponges. *Mar. Ecol. Prog. Ser.* **1991**, *77*, 221–232. [CrossRef]
153. Cimino, G.; Fontana, A.; Giménez, F.; Marin, A.; Mollo, E.; Trivellone, E.; Zubía, E. Biotransformation of a Dietary Sesterterpenoid in the Mediterranean Nudibranch Hypselodoris Orsini. *Experientia* **1993**, *49*, 582–586. [CrossRef]
154. Fontana, A.; Ciavatta, M.L.; DeSouza, L.; Mollo, E.; Naik, C.G.; Parameswaran, P.S.; Wahidullah, S.; Cimino, G. Selected Chemo-Ecological Studies of Marine Opisthobranchs from Indian Coasts. *J. Indian Inst. Sci* **2001**, *81*, 403–415.
155. Gavagnin, M.; Mollo, E.; Docimo, T.; Guo, Y.-W.; Cimino, G. Scalarane Metabolites of the Nudibranch Glossodoris Rufomarginata and Its Dietary Sponge from the South China Sea. *J. Nat. Prod.* **2004**, *67*, 2104–2107. [CrossRef]
156. Wahidullah, S.; Guo, Y.-W.; Fakhr, I.M.I.; Mollo, E. Chemical Diversity in Opisthobranch Molluscs from Scarcely Investigated Indo-Pacific Areas. In *Molluscs: From Chemo-ecological Study to Biotechnological Application*; Cimino, G., Gavagnin, M., Eds.; Progress in Molecular and Subcellular Biology; Springer: Berlin/Heidelberg, Germany, 2006; pp. 175–198, ISBN 978-3-540-30880-5.
157. Manzo, E.; Gavagnin, M.; Somerville, M.J.; Mao, S.-C.; Ciavatta, M.L.; Mollo, E.; Schupp, P.J.; Garson, M.J.; Guo, Y.-W.; Cimino, G. Chemistry of Glossodoris Nudibranchs: Specific Occurrence of 12-Keto Scalaranes. *J. Chem. Ecol.* **2007**, *33*, 2325–2336. [CrossRef]

158. Avila, C.; Durfort, M. Histology of Epithelia and Mantle Glands of Selected Species of Doridacean Molluscs with Chemical Defensive Strategies. *Veliger-Berkeley-* **1996**, *39*, 148–163.
159. Fontana, A.; Mollo, E.; Ricciardi, D.; Fakhr, I.; Cimino, G. Chemical Studies of Egyptian Opisthobranchs: Spongian Diterpenoids from Glossodoris Atromarginata. *J. Nat. Prod.* **1997**, *60*, 444–448. [CrossRef]
160. Haber, M.; Cerfeda, S.; Carbone, M.; Calado, G.; Gaspar, H.; Neves, R.; Maharajan, V.; Cimino, G.; Gavagnin, M.; Ghiselin, M.T.; et al. Coloration and Defense in the Nudibranch Gastropod Hypselodoris Fontandraui. *Biol. Bull.* **2010**, *218*, 181–188. [CrossRef]
161. Sotka, E.E.; Forbey, J.; Horn, M.; Poore, A.G.B.; Raubenheimer, D.; Whalen, K.E. The Emerging Role of Pharmacology in Understanding Consumer–Prey Interactions in Marine and Freshwater Systems. *Integr. Comp. Biol.* **2009**, *49*, 291–313. [CrossRef]
162. Davies, M.S.; Blackwell, J. Energy Saving through Trail Following in a Marine Snail. *Proc. R. Soc. Lond. B Biol. Sci.* **2007**, *274*, 1233–1236. [CrossRef]
163. Winters, A.E.; White, A.M.; Cheney, K.L.; Garson, M.J. Geographic Variation in Diterpene-Based Secondary Metabolites and Level of Defence in an Aposematic Nudibranch, Goniobranchus Splendidus. *J. Molluscan Stud.* **2019**, *85*, 133–142. [CrossRef]
164. Skruber, K.; Read, T.-A.; Vitriol, E.A. Reconsidering an Active Role for G-Actin in Cytoskeletal Regulation. *J. Cell Sci.* **2018**, *131*, 931–933. [CrossRef]
165. Akıl, C.; Tran, L.T.; Orhant-Prioux, M.; Baskaran, Y.; Manser, E.; Blanchoin, L.; Robinson, R.C. Insights into the Evolution of Regulated Actin Dynamics via Characterization of Primitive Gelsolin/Cofilin Proteins from Asgard Archaea. *Proc. Natl. Acad. Sci. USA* **2020**, *117*, 19904–19913. [CrossRef]
166. Boiero Sanders, M.; Antkowiak, A.; Michelot, A. Diversity from Similarity: Cellular Strategies for Assigning Particular Identities to Actin Filaments and Networks. *Open Biol.* **2020**, *10*, 200157. [CrossRef]
167. Akıl, C.; Kitaoku, Y.; Tran, L.T.; Liebl, D.; Choe, H.; Muengsaen, D.; Suginta, W.; Schulte, A.; Robinson, R.C. Mythical Origins of the Actin Cytoskeleton. *Curr. Opin. Cell Biol.* **2021**, *68*, 55–63. [CrossRef]
168. Vedula, P.; Kurosaka, S.; MacTaggart, B.; Ni, Q.; Papoian, G.; Jiang, Y.; Dong, D.W.; Kashina, A. Different Translation Dynamics of β- and γ-Actin Regulates Cell Migration. *eLife* **2021**, *10*, e68712. [CrossRef]
169. Nèeman, I.; Fishelson, L.; Kashman, Y. Isolation of a New Toxin from the Sponge Latrunculia Magnifica in the Gulf of Aquaba (Red Sea). *Mar. Biol.* **1975**, *30*, 293–296. [CrossRef]
170. Edmunds, M. Protective Mechanisms in the Eolidacea (Mollusca Nudibranchia). *Zool. J. Linn. Soc.* **1966**, *46*, 27–71. [CrossRef]
171. Edmunds, M. On the Swimming and Defensive Response of Hexabranchus Marginatus (Mollusca, Nudibranchia). *Zool. J. Linn. Soc.* **1968**, *47*, 425–429. [CrossRef]
172. Ghazali, S.R. Displays of Defense: Behavioral Differences in Antagonist Avoidance in Four Opisthobranch Mollusks. UC Berkeley: UCB Moorea Class: Biology and Geomorphology of Tropical Islands. 2006. Available online: https://escholarship.org/uc/item/9s6740fr (accessed on 30 November 2022).
173. Kistler, H.C.; Broz, K. Cellular Compartmentalization of Secondary Metabolism. *Front. Microbiol.* **2015**, *6*, 68. [CrossRef]
174. Blanco, J. Accumulation of Dinophysis Toxins in Bivalve Molluscs. *Toxins* **2018**, *10*, 453. [CrossRef]
175. Johannes, F.J.; Gallwitz, D. Site-Directed Mutagenesis of the Yeast Actin Gene: A Test for Actin Function in Vivo. *EMBO J.* **1991**, *10*, 3951–3958. [CrossRef]
176. Ujvari, B.; Casewell, N.R.; Sunagar, K.; Arbuckle, K.; Wüster, W.; Lo, N.; O'Meally, D.; Beckmann, C.; King, G.F.; Deplazes, E.; et al. Widespread Convergence in Toxin Resistance by Predictable Molecular Evolution. *Proc. Natl. Acad. Sci. USA* **2015**, *112*, 11911–11916. [CrossRef]
177. Dalla, S.; Dobler, S. Gene Duplications Circumvent Trade-Offs in Enzyme Function: Insect Adaptation to Toxic Host Plants. *Evolution* **2016**, *70*, 2767–2777. [CrossRef]
178. Karageorgi, M.; Groen, S.C.; Sumbul, F.; Pelaez, J.N.; Verster, K.I.; Aguilar, J.M.; Hastings, A.P.; Bernstein, S.L.; Matsunaga, T.; Astourian, M.; et al. Genome Editing Retraces the Evolution of Toxin Resistance in the Monarch Butterfly. *Nature* **2019**, *574*, 409–412. [CrossRef]
179. DesGroseillers, L.; Auclair, D.; Wickham, L. Nucleotide Sequence of an Actin CDNA Gene from Aplysia Californica. *Nucleic Acids Res.* **1990**, *18*, 3654. [CrossRef]
180. Zappulla, J.P.; Angers, A.; Barbas, D.; Castellucci, V.F.; DesGroseillers, L. A Novel Actin Isoform Is Expressed in the Ovotestis of Aplysia Californica. *Comp. Biochem. Physiol. B Biochem. Mol. Biol.* **2005**, *140*, 403–409. [CrossRef]
181. Bryant, M.J.; Flint, H.J.; Sin, F.Y.T. Isolation, Characterization, and Expression Analysis of Three Actin Genes in the New Zealand Black-Footed Abalone, Haliotis Iris. *Mar. Biotechnol. N. Y. N* **2006**, *8*, 110–119. [CrossRef]
182. Sin, F.Y.T.; Bryant, M.J.; Johnstone, A. Molecular Evolution and Phylogeny of Actin Genes in Haliotis Species (Mollusca: Gastropoda). *Zool. Stud.* **2007**, *46*, 734.
183. Ivanov, M.; Todorovska, E.; Radkova, M.; Georgiev, O.; Dolashki, A.; Dolashka, P. Molecular Cloning, Characterization and Phylogenetic Analysis of an Actin Gene from the Marine Mollusk Rapana Venosa (Class Gastropoda). *Int. J. Curr. Microbiol. App. Sci.* **2015**, *4*, 687–700.
184. Adema, C.M.; Hillier, L.W.; Jones, C.S.; Loker, E.S.; Knight, M.; Minx, P.; Oliveira, G.; Raghavan, N.; Shedlock, A.; do Amaral, L.R.; et al. Whole Genome Analysis of a Schistosomiasis-Transmitting Freshwater Snail. *Nat. Commun.* **2017**, *8*, 15451. [CrossRef]

185. Matsunaga, S.; Fusetani, N.; Hashimoto, K.; Koseki, K.; Noma, M.; Noguchi, H.; Sankawa, U. Bioactive Marine Metabolites. 25. Further Kabiramides and Halichondramides, Cytotoxic Macrolides Embracing Trisoxazole, from the Hexabranchus Egg Masses. *J. Org. Chem.* **1989**, *54*, 1360–1363. [CrossRef]
186. Klenchin, V.A.; Allingham, J.S.; King, R.; Tanaka, J.; Marriott, G.; Rayment, I. Trisoxazole Macrolide Toxins Mimic the Binding of Actin-Capping Proteins to Actin. *Nat. Struct. Biol.* **2003**, *10*, 1058–1063. [CrossRef]
187. Tanaka, J.; Yan, Y.; Choi, J.; Bai, J.; Klenchin, V.A.; Rayment, I.; Marriott, G. Biomolecular Mimicry in the Actin Cytoskeleton: Mechanisms Underlying the Cytotoxicity of Kabiramide C and Related Macrolides. *Proc. Natl. Acad. Sci. USA* **2003**, *100*, 13851–13856. [CrossRef]
188. Parrish, S.M.; Yoshida, W.; Yang, B.; Williams, P.G. Ulapualides C–E Isolated from a Hawaiian Hexabranchus Sanguineus Egg Mass. *J. Nat. Prod.* **2017**, *80*, 726–730. [CrossRef]
189. Yamada, K.; Ojika, M.; Ishigaki, T.; Yoshida, Y.; Ekimoto, H.; Arakawa, M. Aplyronine A, a Potent Antitumor Substance and the Congeners Aplyronines B and C Isolated from the Sea Hare Aplysia Kurodai. *J. Am. Chem. Soc.* **1993**, *115*, 11020–11021. [CrossRef]
190. Saito, S.; Watabe, S.; Ozaki, H.; Kigoshi, H.; Yamada, K.; Fusetani, N.; Karaki, H. Novel Actin Depolymerizing Macrolide Aplyronine A1. *J. Biochem.* **1996**, *120*, 552–555. [CrossRef]
191. Ojika, M.; Kigoshi, H.; Yoshida, Y.; Ishigaki, T.; Nisiwaki, M.; Tsukada, I.; Arakawa, M.; Ekimoto, H.; Yamada, K. Aplyronine A, a Potent Antitumor Macrolide of Marine Origin, and the Congeners Aplyronines B and C: Isolation, Structures, and Bioactivities. *Tetrahedron* **2007**, *63*, 3138–3167. [CrossRef]
192. Kigoshi, H.; Kita, M. Antitumor Effects of Sea Hare-Derived Compounds in Cancer. In *Handbook of Anticancer Drugs from Marine Origin*; Kim, S.-K., Ed.; Springer International Publishing: Cham, Switzerland, 2015; pp. 701–739, ISBN 978-3-319-07145-9.
193. Hughes, C.C.; Fenical, W. Antibacterials from the Sea. *Chem. Weinh. Bergstr. Ger.* **2010**, *16*, 12512–12525. [CrossRef]
194. Ueoka, R.; Uria, A.R.; Reiter, S.; Mori, T.; Karbaum, P.; Peters, E.E.; Helfrich, E.J.N.; Morinaka, B.I.; Gugger, M.; Takeyama, H.; et al. Metabolic and Evolutionary Origin of Actin-Binding Polyketides from Diverse Organisms. *Nat. Chem. Biol.* **2015**, *11*, 705–712. [CrossRef]